

A unified performance analysis of likelihood-informed subspace methods

TIANGANG CUI¹, XIN T. TONG²

¹Monash University, School of Mathematics E-mail: tiangang.cui@monash.edu

²National University of Singapore, Department of Mathematics E-mail: mattxin@nus.edu.sg

The likelihood-informed subspace (LIS) method offers a viable route to reducing the dimensionality of high-dimensional probability distributions arising in Bayesian inference. LIS identifies an intrinsic low-dimensional linear subspace where the target distribution differs the most from some tractable reference distribution. Such a subspace can be identified using the leading eigenvectors of a Gram matrix of the gradient of the log-likelihood function. Then, the original high-dimensional target distribution is approximated through various forms of marginalization of the likelihood function, in which the approximated likelihood only has support on the intrinsic low-dimensional subspace. This approximation enables the design of inference algorithms that can scale sub-linearly with the apparent dimensionality of the problem. Intuitively, the accuracy of the approximation, and hence the performance of the inference algorithms, are influenced by three factors—the dimension truncation error in identifying the subspace, Monte Carlo error in estimating the Gram matrices, and Monte Carlo error in constructing marginalizations. This work establishes a unified framework to analyze each of these three factors and their interplay. Under mild technical assumptions, we establish error bounds for a range of existing dimension reduction techniques based on the principle of LIS. Our error bounds also provide useful insights into the accuracy of these methods. In addition, we analyze the integration of LIS with sampling methods such as Markov Chain Monte Carlo (MCMC) and sequential Monte Carlo (SMC). We also demonstrate the applicability of our analysis on a linear inverse problem with Gaussian prior, which shows that all the estimates can be dimension-independent if the prior covariance is a trace-class operator. Finally, we demonstrate various aspects of our theoretical claims on two nonlinear inverse problems.

Keywords: Dimension reduction; Approximation error; Likelihood informed subspace; Monte Carlo estimation

1. Introduction

Many applications in science and engineering must contend with expensive or intractable models that are typically driven by high-dimensional or even infinite-dimensional random variables. Some examples are seismic imaging [16, 42], subsurface energy [22], glaciology [49], groundwater [28, 34], electrical impedance tomography [35], and density estimation [46]. Denoting the high-dimensional random variables of interest by $X \in \mathcal{X} \subseteq \mathbb{R}^d$, the associated target probability density often takes the form

$$\pi(x) = \frac{1}{Z} \mu(x) f(x), \quad Z = \int \mu(x) f(x) dx, \quad (1)$$

where we refer to Z , $\mu(x)$, and $f(x)$ as the *normalization constant*, the *reference density* and the *likelihood function*, respectively. In the most common scenario, the target density is the posterior defined by Bayes' rule, the reference density is the prior, and the likelihood function is often denoted by $f(x; y)$ for some observed data y . Here we drop the dependency of f on y for brevity unless otherwise required.

In most of the aforementioned applications, the reference density $\mu(x)$ takes a simple form, e.g. a Gaussian density or an elliptical density, so that the reference distribution, its marginal distributions, and its conditional distributions can be directly evaluated and sampled from. However, the likelihood

function f , which often encodes some highly nonlinear parameter-to-observable map that represents the underlying model, may introduce complicated nonlinear interactions among parameters. When the parameter is also high-dimensional, generating samples from the target distribution using classical methods such as Markov chain Monte Carlo (MCMC) and sequential Monte Carlo (SMC) can be a computationally challenging task. The computational effort required for generating each independent sample from $\pi(x)$ may scale super-linearly with the ambient parameter dimension d .

In many high-dimensional problems, there often exists a low-dimensional “effective” or “intrinsic” dimension. Designing scalable sampling methods that can use this property has been a focus in the recent literature [1, 2, 3, 6, 7, 8, 23, 45, 51, 52, 61]. One effective strategy involves finding a parameter subspace \mathcal{X}_r with dimensionality $d_r \ll d$, so that the original density with high ambient parameter dimensions can be approximated by some low-dimensional parametrization. The recently developed likelihood informed subspace (LIS) method [19, 25, 65] offers a way to identify \mathcal{X}_r for high-dimensional target densities and approximates the target density via projections of the likelihood function onto \mathcal{X}_r . For sampling related problems, such projections naturally lead to MCMC and SMC computations on the reduced subspace \mathcal{X}_r . As a result, this may significantly lower the computation effort compared with implementations directly targeting the ambient space \mathcal{X} . In this work, we focus on the analysis of the approximation accuracy of the LIS method and its related sampling algorithms.

1.1. Likelihood informed subspaces

Dimension reduction techniques have been exploited to reduce the computational cost due to the parameter dimension. When the target density $\pi(x)$ has a known covariance matrix Σ , a common approach is to use the principal component analysis or Karhunen–Loève decomposition [36, 41] that identifies the leading eigenvectors of Σ to define the subspace \mathcal{X}_r . Then, the parameters in the complement subspace of \mathcal{X}_r are ignored in the inference problem. Other than the computational difficulties of estimating the covariance matrix for high-dimensional non-Gaussian target densities, this approach is proven to be suboptimal even for problems with Gaussian reference densities and Gaussian likelihood functions [54].

Without ignoring parameters from the inference procedure, LIS exploits an alternative way to approximate target densities. The intuition underpinning the development of LIS is that the likelihood function $f(x_r, x_\perp)$ is often effectively supported on a low-dimensional subspace \mathcal{X}_r with dimension $d_r \ll d$. In other words, f can be approximated by a function that depends only on $x_r \in \mathcal{X}_r$. For a given subspace \mathcal{X}_r with dimension d_r , we denote its complement subspace by \mathcal{X}_\perp and define projection operators P_r and P_\perp such that $\text{range}(P_r) = \mathcal{X}_r$ and $\text{range}(P_\perp) = \mathcal{X}_\perp$. A parameter x can be decomposed as

$$x = x_r + x_\perp, \quad x_r = P_r x \in \mathcal{X}_r, \quad x_\perp = P_\perp x \in \mathcal{X}_\perp. \quad (2)$$

For a density $\nu(x_r, x_\perp)$ on \mathbb{R}^d , we use $\bar{\nu}(x_r)$ to denote its marginal on \mathcal{X}_r and $\nu(x_\perp|x_r)$ to denote the conditional density. This way, the target density can be decomposed as

$$\pi(x) \equiv \pi(x_r, x_\perp) = \bar{\pi}(x_r)\pi(x_\perp|x_r),$$

where the marginal density and the conditional density take the form

$$\bar{\pi}(x_r) = \frac{1}{Z} \bar{\mu}(x_r) \int f(x_r, x_\perp) \mu(x_\perp|x_r) dx_\perp \quad \text{and} \quad \pi(x_\perp|x_r) = \frac{f(x_r, x_\perp) \mu(x_\perp|x_r)}{\int f(x_r, x_\perp) \mu(x_\perp|x_r) dx_\perp}, \quad (3)$$

respectively. With the assumption that the likelihood function f is effectively supported on \mathcal{X}_r , the above decomposition suggests that $\mu(x_\perp|x_r)$ can be a good approximation of $\pi(x_\perp|x_r)$. Thus, one

can identify the subspace \mathcal{X}_r and construct a suitable *lower-dimensional surrogate* density $\bar{\varphi}_s(x_r)$ to approximate the marginal target density $\bar{\pi}(x_r)$. This allows one to approximate the full-dimensional target density by

$$\varphi_s(x_r, x_\perp) \propto \bar{\varphi}_s(x_r)\mu(x_\perp|x_r), \quad (4)$$

where the subscript s in $\bar{\varphi}_s(x_r)$ and $\varphi_s(x_r, x_\perp)$ denotes the method for constructing the surrogate density, which will be specified in Section 1.2. The approximate target density $\varphi_s(x_r, x_\perp)$ can be efficiently sampled using a two-step strategy—one can first apply MCMC or SMC to generate samples from the lower-dimensional surrogate density $\bar{\varphi}_s(x_r)$, and then draw independent samples from the conditional reference density $\mu(x_\perp|x_r)$.

The identification of the subspace \mathcal{X}_r is the key in constructing approximate densities in the form of (4). Several methods based on the derivative information of the likelihood function have been developed for this purpose. Some examples include the use of the Fisher information matrix [25, 24], the Hessian matrix of $\log f$ [17, 42], and the gradient of $\log f$ [19, 65]. Here we focus on the analysis of the gradient-based techniques. Note that the gradient of the logarithm of the likelihood, $\nabla \log f(x)$, indicates a local direction at x in which the log-likelihood changes most rapidly, and the Gram matrix of $\nabla \log f(X)$ after averaging over all outcomes of X can measure variations of the likelihood function. Depending on the choice of the distribution assigned to X , different Gram matrices have been considered:

$$\begin{aligned} H_0 &:= \int \nabla \log f(x) \nabla \log f(x)^\top \mu(x) dx, \\ H_1 &:= \int \nabla \log f(x) \nabla \log f(x)^\top \pi(x) dx. \end{aligned} \quad (5)$$

When the gradient Gram matrix H_k , $k \in \{0, 1\}$, is presented, the subspace spanned by the eigenvectors of the largest eigenvalues of H_k preserves most of the variations of $\nabla \log f(x)$. Thus, the first d_r eigenvectors (which we will refer to as the ‘leading eigenvectors’) of the gradient Gram matrix can be used to construct the subspace \mathcal{X}_r .

Both H_0 and H_1 can be numerically estimated using Monte Carlo integration. The matrix H_0 can be simply estimated using independent samples drawn from the reference density $\mu(x)$. In comparison, estimation of H_1 is more challenging, because samples drawn from the target density $\pi(x)$ are needed. One may apply importance sampling

$$H_1 = \frac{1}{Z} \int \nabla \log f(x) \nabla \log f(x)^\top f(x) \mu(x) dx,$$

so that samples from $\mu(x)$ weighted by the likelihood function can be used to estimate H_1 . However, the likelihood $f(x)$ may concentrate in a small region for problems with informative data, and thus the above importance sampling formula may suffer from a low effective sample size. In this case, adaptive MCMC sampling or SMC sampling can be used to estimate H_1 . At first glance, it appears that the matrix H_1 is not an effective way to identify the subspace \mathcal{X}_r . However, our analysis explains why using H_1 instead of H_0 leads to a more accurate approximation of the subspace \mathcal{X}_r .

1.2. Posterior approximation via marginalization

Given a subspace \mathcal{X}_r , here we discuss three methods for building the lower-dimensional surrogate density. A natural choice is to use the marginal density in (3).

Definition 1.1 (Marginal likelihood). *By marginalizing the likelihood function over the complement subspace \mathcal{X}_\perp , one has*

$$\bar{f}(x_r) := \int f(x_r, x_\perp) \mu(x_\perp | x_r) dx_\perp = \mathbb{E}_\mu(f(X) | P_r X = x_r). \quad (6)$$

This yields the lower-dimensional surrogate density $\bar{\varphi}_f(x_r) = \frac{1}{Z} \bar{f}(x_r) \mu(x_r)$ and the approximate target density $\varphi_f(x_r, x_\perp) = \bar{\varphi}_f(x_r) \mu(x_\perp | x_r)$.

Since the low-dimensional surrogate density $\bar{\varphi}_f(x_r)$ is equivalent to the marginal target density $\bar{\pi}(x_r)$, the approximate target density φ_f shares the same normalizing constant Z with the full-dimensional target π . Closely related to the marginal likelihood approximation, we also consider the following approximations based on marginalizing the square root of the likelihood and the logarithm of the likelihood.

Definition 1.2 (Radical likelihood). *Defining the square root of the likelihood by $g(x) := \sqrt{f(x)}$, the marginal function $\bar{g}(x_r) = \mathbb{E}_\mu(g(X) | P_r X = x_r)$ defines the lower-dimensional surrogate density*

$$\bar{\varphi}_g(x_r) = \frac{1}{Z_g} \bar{g}(x_r)^2 \mu(x_r), \quad Z_g = \int \bar{g}(x_r)^2 \mu(x_r) dx_r, \quad (7)$$

and the approximate target density $\varphi_g(x_r, x_\perp) = \bar{\varphi}_g(x_r) \mu(x_\perp | x_r)$.

Definition 1.3 (Log-likelihood). *Defining the logarithm of the likelihood by $l(x) := \log f(x)$, the marginal function $\bar{l}(x_r) = \mathbb{E}_\mu(l(X) | P_r X = x_r)$ defines the lower-dimensional surrogate density*

$$\bar{\varphi}_l(x_r) = \frac{1}{Z_l} \exp(\bar{l}(x_r)) \mu(x_r), \quad Z_l = \int \exp(\bar{l}(x_r)) \mu(x_r) dx_r, \quad (8)$$

and the approximate target density $\varphi_l(x_r, x_\perp) = \bar{\varphi}_l(x_r) \mu(x_\perp | x_r)$.

Note that the combination of φ_l and the subspace defined by H_0 is also known as the *active subspace* method [19] in the literature. To provide a unified discussion, here we view it as one specific scenario of the LIS. While using φ_g and φ_l may seem less natural than using φ_f , we will show in Sections 2-4 that their theoretical and computational properties differ from those of φ_f . We use the shorthand notation $X \sim \mu(x)$ to indicate that a random variable X follows a probability distribution with the density $\mu(x)$. In practice, we can generate independent and identically distributed (i.i.d.) samples $X_\perp^i | X_r = x_r, i = 1, \dots, M$, from the conditional distribution $\mu(x_\perp | x_r)$ using a map $X_\perp^i = T(x_r, W^i)$, where W^i are i.i.d. samples describing the randomness of X_\perp conditioned on X_r . Then the marginalization in all of the approximate likelihood functions $\bar{f}(x_r)$, $\bar{g}(x_r)$, and $\bar{l}(x_r)$ can be respectively computed by Monte Carlo integration

$$\bar{f}^M(x_r) := \frac{1}{M} \sum_{i=1}^M f(x_r, X_\perp^i), \quad \bar{g}^M(x_r) := \frac{1}{M} \sum_{i=1}^M g(x_r, X_\perp^i), \quad \bar{l}^M(x_r) := \frac{1}{M} \sum_{i=1}^M l(x_r, X_\perp^i). \quad (9)$$

Then, we denote the corresponding Monte Carlo version of the densities by

$$\bar{\varphi}_f^M(x_r) \propto \bar{f}^M(x_r) \mu(x_r), \quad \bar{\varphi}_g^M(x_r) \propto \bar{g}^M(x_r)^2 \mu(x_r), \quad \bar{\varphi}_l^M(x_r) \propto \exp(\bar{l}^M(x_r)) \mu(x_r),$$

respectively, and the corresponding Monte Carlo version of the approximate target densities in a similar way.

1.3. Related work and main contributions

The use of the approximate target densities naturally introduces errors compared with solutions obtained from the full target densities. Several interconnected factors impact the approximation accuracy. Under mild assumptions, this paper aims to assess the following error sources and the performance of related sampling algorithms:

1. **Accuracy of $\varphi_s(x)$, $s \in \{f, g, l\}$.** In Section 2, we derive error bounds on the difference between the approximate target densities φ_s and the full-dimensional target π , quantified through either estimation error of some test function or various statistical divergences. The highlight is that all these errors can all be bounded by the spectrum of H_0 or H_1 . So if we have the true values of H_0 or H_1 , we can find the optimal projection subspace with performance guarantees. From the results, we will also observe that the approximation error of the subspace estimated using H_1 tends to be smaller than that of the subspace estimated using H_0 , and it is independent of the normalizing constant. In subspace estimation, this leads to a trade-off between H_0 and H_1 : the former is easier to estimate while the latter tends to have better approximation accuracy.
2. **Monte Carlo errors of $\varphi_s^M(x)$, $s \in \{f, g, l\}$.** In most practical cases, each of the approximate target densities $\varphi_s(x)$ need to be replaced by the Monte Carlo version $\varphi_s^M(x)$ using samples drawn from the conditional reference density $\mu(x_\perp|x_r)$. In Section 3, we show that Monte Carlo averaging incurs an additional error that is about $O(1/\sqrt{M})$ times as large as the error of $\varphi_s(x)$. Therefore, M can be small when the approximation error of $\varphi_s(x)$ is moderate.
3. **Monte Carlo errors in estimating H_0 and H_1 .** The Gram matrices H_0 and H_1 must be approximated by their Monte Carlo estimates \hat{H}_0 and \hat{H}_1 , respectively. The resulting sample-averaged subspace $\hat{\mathcal{X}}_r$ may lead to additional approximation errors. In Section 4, we establish bounds on the errors of the approximate target densities using $\hat{\mathcal{X}}_r$ instead of using the true subspace \mathcal{X}_r . These bounds only depend on the dimension of $\hat{\mathcal{X}}_r$ and the variances of H_0 and H_1 . Importantly, our bounds do not rely on eigenvalue gaps, which is a typical assumption used in dimension reduction (e.g., [19]) but may have limited practical applicability. See Remark 4.4, Figures 1 and 6, and [29] for further details.
4. **Efficiency of LIS accelerated sampling.** We can implement MCMC to draw samples from the low-dimensional surrogate density $\bar{\varphi}_s(x_r)$, and then augment the low-dimensional samples by adding samples drawn from the conditional reference density $\mu(x_\perp|x_r)$ to obtain samples from the full-dimensional approximate target density $\varphi_s(x)$. In Section 5.1, we investigate the efficiency of this algorithm, in which Proposition 5.1 shows the overall efficiency is mostly determined by the MCMC targeting the approximate target density $\varphi_s(x_r)$. In Section 5.2, we further investigate the connection between SMC and LIS, in particular how to use SMC to simplify the estimation of H_1 .
5. **Dimension independence.** LIS methods are mostly used in high-dimensional problems, and hence it is important for the error bounds to be dimension independent. In other words, various approximation error bounds should depend only on the effective dimension d_r and some other statistics, but not on the ambient dimension d . We illustrate this is indeed the case in Section 6 for a class of linear inverse problems. It also serves as a concrete example to demonstrate the efficacy of our analysis.

We provide some numerical examples on nonlinear inverse problems to further verify our results in Section 7. We allocate most of the technical proofs to the Appendix.

We now discuss some related work that addresses the preceding issues. In [19], Problems 1–3 are investigated in the context of the active subspace method, which employs φ_l with \mathcal{X}_r estimated from H_0 , using the Hellinger distance. An analysis similar to that of [19] has also been developed for function approximation problems with H_0 in [48]. The work of [65] investigated Problems 1–3 for φ_f

with \mathcal{X}_r estimated from H_1 using the Kullback–Leibler (KL) divergence. For Problem 1, our analysis establishes new error bounds of $\varphi_s, s \in \{f, g\}$ with \mathcal{X}_r estimated from both H_1 and H_0 based on the Hellinger distance. Using the bounds on the Hellinger errors, we can establish new sharp bounds on the expected Monte Carlo errors in $\varphi_s^M, s \in \{f, g\}$ for Problem 2. This analysis also sheds light on the trade-off between H_0 and H_1 . For the sake of completeness, we also establish the error bound of φ_l and φ_l^M with \mathcal{X}_r estimated from H_0 based on the KL divergence. Moreover, our analysis for Problem 3 does not require the eigenvalue gap condition, which is assumed in [19, 65] and not easily fulfilled in applications (see Remark 4.4, Figures 1 and 6 and [29]). Low-rank matrix approximation methods that do not require an eigenvalue gap have also been studied, e.g. in [29], but not for sample-averaged subspace estimation. Beyond Problems 1–3, our analysis also enables us to investigate Problems 4 and 5, which have practical significance but have not been previously addressed.

2. Accuracy of approximate target densities

Our starting point is to establish bounds on the errors of approximate target densities $\varphi_s(x), s \in \{f, g, l\}$ in Section 1.2. We consider two forms to quantify the approximation errors. The first way is through the estimation error. Suppose the goal is to estimate $\mathbb{E}_\pi[h]$ for some function of interest h . The approximate density φ_s yields an approximate estimate $\mathbb{E}_{\varphi_s}[h]$ that has the estimation error

$$\mathcal{E}_h(\pi, \varphi_s) := |\mathbb{E}_\pi[h] - \mathbb{E}_{\varphi_s}[h]|. \quad (10)$$

The second way is via statistical divergences, which are also known as f -divergences. Some popular choices include the (squared) Hellinger distance

$$D_H(\pi, \nu)^2 = \frac{1}{2} \int \left(\sqrt{\frac{\pi(x)}{\lambda(x)}} - \sqrt{\frac{\nu(x)}{\lambda(x)}} \right)^2 \lambda(x) dx.$$

where λ is a reference density such as the Lebesgue density; and the KL divergence

$$D_{KL}(\pi, \nu) = \int \log \frac{\pi(x)}{\nu(x)} \pi(x) dx.$$

We present in Lemma A.1 a few results regarding the relationship between these divergences and their connections with the estimation error \mathcal{E}_h . Various error forms can be useful for applying dimension reduction in different inference tasks, as each inference task often has its “preferred” way to quantify the error. For example, the optimization problems in transport maps [9, 43, 53] and Stein variational methods [27, 40] are formulated using the KL divergence, tensor train [21] and other approximation methods, e.g., [39], give bounds in terms of the Hellinger distance, and the min-max formulation in density estimation methods such as [59, 60, 62] relies on the estimation error in (10). Unless otherwise specified, we only consider the estimation error and statistical divergences of the full-dimensional approximate target densities $\varphi_s(x), s \in \{f, g, l\}$ rather than their lower-dimensional counterparts $\bar{\varphi}_s(x_r)$.

For different combinations of approximate target densities, $\varphi_s(x), s \in \{f, g, l\}$, and subspace construction methods, $H_k, k \in \{0, 1\}$, our first result discusses the *a priori* estimate of either $\mathcal{E}_h(\pi, \varphi_s)$ or $D_{(\cdot)}(\pi, \varphi_s)$ using the subspace \mathcal{X}_r and spectral information of H_k . Intuitively, the approximation error is related to the sum of the residual eigenvalues of H_k , which is denoted by

$$\mathcal{R}(\mathcal{X}_r, H_k) := \text{tr}(P_\perp H_k P_\perp), \quad (11)$$

where P_\perp is the projector defined in (2). Note that (11) is well defined for any linear subspace \mathcal{X}_r and computable for a given H_k , whereas many statistical divergences do not have closed-form formulas.

To build a connection between approximation errors of $\varphi_s(x)$ and the residual function $\mathcal{R}(\mathcal{X}_r, H_k)$, we assume the reference density $\mu(x)$ is compatible with the subspace \mathcal{X}_r in the following sense:

Assumption 2.1. *The conditional reference density $\mu(x_\perp|x_r)$ satisfies a κ -Poincaré inequality: for all x_r and any \mathbb{C}^1 function h :*

$$\text{var}_{\mu(x_\perp|x_r)}(h) \leq \kappa \int \|\nabla h(x_r, x_\perp)\|^2 \mu(x_\perp|x_r) dx_\perp.$$

Assumption 2.1 asserts a Poincaré-type inequality that is modified for our subspace approximations. In probability theory, it is well known that Poincaré-type inequalities hold for any strongly log-concave density $\mu(x)$. We refer the readers to [10] for a summary and its connection to other inequalities such as the Brascamp–Lieb inequality [15] and the logarithmic Sobolev inequality [12, 31, 38, 47]. In the following proposition, we provide a concrete example of Assumption 2.1 for the case that $\mu(x)$ is a slight perturbation from a strongly log-concave density. A similar result can be found in [65, Corollary F.4]. We provide it here for the sake of completeness.

Proposition 2.2. *Suppose $\mu(x) \propto \exp(-V(x) - U(x))$ and there are constants $c, B > 0$ such that*

- *For any x , the minimal eigenvalue of the Hessian $\nabla^2 V(x)$ is larger than c ;*
- *The variation in U is bounded in the sense that $\exp(\sup_x U(x) - \inf_x U(x)) \leq B$;*

Then Assumption 2.1 holds with $\kappa = B^2/c$.

Proof. See Appendix B.1. □

Table 1. A summary of approximation error bounds. The second column indicates the functions marginalized by the approximate target densities.

approximation method	marginalization	approximation errors	upper bounds
H_1 and φ_f	f	$\mathcal{E}_h, D_H, (\sqrt{D_{KL}})$	$O(\mathcal{R}(\mathcal{X}_r, H_1)^{\frac{1}{2}})$
H_1 and φ_g	$g = \sqrt{f}$	\mathcal{E}_h, D_H	$O(\mathcal{R}(\mathcal{X}_r, H_1)^{\frac{1}{2}})$
H_0 and φ_f	f	\mathcal{E}_h, D_H	$O(\mathcal{R}(\mathcal{X}_r, H_0)^{\frac{1}{2}})$
H_0 and φ_g	$g = \sqrt{f}$	\mathcal{E}_h, D_H	$O(\mathcal{R}(\mathcal{X}_r, H_0)^{\frac{1}{2}})$
H_0 and φ_l	$l = \log f$	$\mathcal{E}_h, D_H, \sqrt{D_{KL}}$	$O(\mathcal{R}(\mathcal{X}_r, H_0)^{\frac{1}{4}})$

Under Assumption 2.1 we will show that $\mathcal{E}_h(\pi, \varphi_s)$ and $D_{(\cdot)}(\pi, \varphi_s)$ can be upper bounded by a fractional power of $\mathcal{R}(\mathcal{X}_r, H_k)$. We summarize the results in Table 1. The first row indicates that if the Gram matrix H_1 and the approximate density φ_f are used, then $\mathcal{E}_h(\pi, \varphi_f)$ is bounded by $O(\sqrt{\mathcal{R}(\mathcal{X}_r, H_1)})$. The same applies to other entries in the table. Note that we have written parentheses around $\sqrt{D_{KL}}$ for H_1 and φ_f , since this scenario has been analyzed in [65] under a similar

assumption. Therefore we do not discuss bounds for $D_{KL}(\pi, \varphi_f)$ and focus on other bounds that have yet to be analyzed. We first consider the approximations (H_1, φ_f) and (H_1, φ_g) as described in Definitions 1.1 and 1.2, respectively.

Proposition 2.3. *For a given subspace \mathcal{X}_r , the expected conditional variance of the radical likelihood function $g = \sqrt{f}$ provides the following upper bounds:*

$$\begin{aligned} 1) \quad D_H(\pi, \varphi_f)^2 &\leq \frac{1}{Z} \int \text{var}_{\mu(x_\perp|x_r)}[g] \mu(x_r) dx_r. \\ 2) \quad D_H(\pi, \varphi_g)^2 &\leq \frac{1}{Z} \int \text{var}_{\mu(x_\perp|x_r)}[g] \mu(x_r) dx_r. \end{aligned}$$

In addition, the normalizing constants Z and Z_g satisfy $Z \geq Z_g$.

Proof. See Appendix B.2. □

Theorem 2.4. *Suppose the approximate densities φ_f and φ_g are obtained using a subspace \mathcal{X}_r constructed from the matrix H_1 . Under Assumption 2.1, we have the following:*

1) *The Hellinger distance between π and φ_f is bounded by*

$$D_H(\pi, \varphi_f) \leq \frac{1}{2} \sqrt{\kappa \mathcal{R}(\mathcal{X}_r, H_1)}. \quad (12)$$

2) *The estimation error with any L^2 integrable function h is given by*

$$\mathcal{E}_h(\pi, \varphi_f) \leq \sqrt{\frac{\kappa}{2} (\mathbb{E}_\pi[h^2] + \mathbb{E}_{\varphi_f}[h^2]) \mathcal{R}(\mathcal{X}_r, H_1)}.$$

3) *The above two claims also hold for the approximation φ_g .*

Proof. See Appendix B.3. □

Although the result of Theorem 2.4 claim 1) can also be obtained from Lemma A.1 claim 2) and Corollary 1 of [65] (which uses the logarithmic Sobolev inequality), our proof offers additional insights into the subspace construction. Proposition 2.3 connects the error of approximate target densities with the κ -Poincaré inequality via the expected conditional variance. This may also lead to new subspace construction techniques beyond the gradient-based methods.

Remark 2.5. *Recalling the definitions of H_k , we have $H_1 \leq \frac{1}{Z} \sup_x f H_0$. Thus, we have a direct corollary of Theorem 2.4 for the case where the subspace \mathcal{X}_r is constructed from the matrix H_0 :*

$$D_H(\pi, \varphi_f) \leq \frac{1}{2} \sqrt{\frac{\kappa \sup_x f}{Z} \mathcal{R}(\mathcal{X}_r, H_0)}, \quad D_H(\pi, \varphi_g) \leq \frac{1}{2} \sqrt{\frac{\kappa \sup_x f}{Z} \mathcal{R}(\mathcal{X}_r, H_0)}. \quad (13)$$

Similar bounds for the L^2 distance between $\log \varphi_l$ and $\log \pi$ assuming $\sup_x f = 1$ can be found in Theorem 3.1 [19] with a more complicated pre-constant. In problems where the likelihood function f concentrates in a small region, the associated normalizing constant Z can be small. This way, the constant on the right-hand side of (13) can have a large value. In contrast, the only constant in (12) is κ , which is of value 0.5 when the reference density is the standard Gaussian distribution. This partially explains why using H_0 can be suboptimal. Following this observation, we predict that the reduced subspace from H_1 will perform better than the one from H_0 , especially when the likelihood function has concentrated support. This will be verified in our numerical examples.

For the approximate target density φ_l , one can obtain bounds on the associated approximation errors only if the matrix H_0 is used to construct the subspace. In contrast, for the approximate target densities φ_f and φ_g , error bounds can be obtained using both H_1 and H_0 . See Table 1. The error bounds for φ_l are in general weaker than those for φ_f and φ_g —they depend on additional constants that can take large values and the exponent of $\mathcal{R}(\mathcal{X}_r, H_0)$ in the error bounds is $1/4$.

Theorem 2.6. *Suppose the approximate density φ_l is obtained using a subspace \mathcal{X}_r constructed from the matrix H_0 . Under Assumption 2.1, we have the following:*

1) *The error in KL-divergence is bounded by*

$$D_{KL}(\pi, \varphi_l) \leq \frac{\sqrt{\kappa} \|f\|_{2,\mu}}{Z} \sqrt{\mathcal{R}(\mathcal{X}_r, H_0)}, \quad \|f\|_{2,\mu} := \sqrt{\int f^2(x) \mu(x) dx} \geq Z.$$

This also leads to an upper bound in Hellinger distance, since $D_H(\pi, \varphi_l) \leq \sqrt{\frac{1}{2} D_{KL}(\pi, \varphi_l)}$.

2) *The estimation error is bounded by*

$$|\mathbb{E}_\pi[h] - \mathbb{E}_{\varphi_l}[h]| \leq (\mathbb{E}_\pi[h^2] + \mathbb{E}_{\varphi_l}[h^2])^{\frac{1}{2}} \sqrt{\frac{\|f\|_{2,\mu}}{Z} (\kappa \mathcal{R}(\mathcal{X}_r, H_0))^{\frac{1}{4}}}.$$

Proof. See Appendix B.4. □

3. Monte Carlo error of approximate target densities

To construct the approximate densities $\varphi_s, s \in \{f, g, l\}$, the marginalization in the lower-dimensional likelihood approximations (cf. Definitions 1.1–1.3) often needs to be computed by Monte Carlo integration, where i.i.d. samples $X_\perp^i | X_r = x_r, i = 1, \dots, M$, drawn from the conditional reference density $\mu(x_\perp | x_r)$ are used. To estimate the expected errors of the Monte Carlo version of the approximate densities, denoted by $\varphi_s^M, s \in \{f, g, l\}$, we consider the expectation of some function in the form of

$$h^M := \int h(x_r, X_\perp^1, \dots, X_\perp^M) \bar{\mu}(x_r) dx_r.$$

By generating conditional samples from $\mu(x_\perp | x_r)$ using a map $X_\perp = T(x_r, W)$, where $W \sim \nu(w)$, we can express the expectation of h^M over all possible outcomes of $X_\perp^i | X_r = x_r, i = 1, \dots, M$, as

$$\mathbb{E}_M [h^M] := \int \dots \int h(x_r, T(x_r, w^1), \dots, T(x_r, w^M)) \bar{\mu}(x_r) dx_r \left(\prod_{i=1}^M \nu(w^i) \right) dw^1 \dots dw^M,$$

in order to remove the conditional dependency of X_\perp^i on X_r in the expectation. The following theorems reveal the accuracy of the sample-averaged approximate densities φ_s^M .

Theorem 3.1. *Suppose the approximate densities φ_f and φ_g are obtained using a subspace \mathcal{X}_r constructed from the matrix H_1 . Under Assumption 2.1, the following bounds hold:*

1) *The expected Hellinger distance between φ_g^M and φ_f satisfies*

$$\mathbb{E}_M [D_H(\varphi_g^M, \varphi_f)] \leq \frac{\sqrt{2\kappa Z}}{\sqrt{Z_g M}} \sqrt{\mathcal{R}(\mathcal{X}_r, H_1)}.$$

2) Given the conditional likelihood $f(x_\perp|x_r) := f(x_\perp, x_r)/\bar{f}(x_r)$ and $C_f = \sup_{x_r} \sup_{x_\perp} f(x_\perp|x_r)$, then the expected Hellinger distance between φ_f^M and φ_f satisfies

$$\mathbb{E}_M \left[D_H(\varphi_f^M, \varphi_f) \right] \leq \frac{\sqrt{2\kappa C_f}}{\sqrt{M}} \sqrt{\mathcal{R}(\mathcal{X}_r, H_1)}.$$

Proof. See Appendix C.1. □

Note that claim 2) of Theorem 3.1 needs an additional assumption on the supremum of $f(x_\perp|x_r)$, while claim 1) does not, showing the analytical advantage of φ_g . The requirement that $f(x_\perp|x_r)$ is bounded is not restrictive in practice, since the conditional likelihood is expected to be flat in the complement subspace of \mathcal{X}_r . Since the Hellinger distance enjoys the triangle inequality, we have

$$\mathbb{E}_M \left[D_H(\varphi_s^M, \pi) \right] \leq \mathbb{E}_M \left[D_H(\varphi_s^M, \varphi_s) \right] + D_H(\varphi_s, \pi), \quad s \in \{f, g\}.$$

This way, Theorem 3.1 and Theorem 2.4 together reveal that the Monte Carlo averaging used in $\varphi_s^M(x)$, $s \in \{f, g\}$ incurs an additional error that is about $O(1/\sqrt{M})$ as large as the error of $\varphi_s(x)$, $s \in \{f, g\}$. Since the KL-divergence does not satisfy the triangle inequality, we directly establish the bound on $\mathbb{E}_M \left[D_{KL}(\pi, \varphi_l^M) \right]$ as follows.

Theorem 3.2. *Suppose the approximate density φ_l is obtained using a subspace \mathcal{X}_r constructed from the matrix H_0 . Under Assumption 2.1, the expected L^2 error of the marginalized log-likelihood is bounded by*

$$\mathbb{E}_M \left[\left(\int (\bar{l}^M(x_r) - \bar{l}(x_r))^2 \mu(x_r) dx_r \right)^{\frac{1}{2}} \right] \leq \frac{\sqrt{\kappa}}{\sqrt{M}} \sqrt{\mathcal{R}(\mathcal{X}_r, H_0)}.$$

The expected KL-divergence of π from the approximation φ_l^M is bounded by

$$\mathbb{E}_M \left[D_{KL}(\pi, \varphi_l^M) \right] \leq \frac{\sqrt{\kappa} \|f\|_{2, \mu}}{Z} \left(1 + \frac{1}{\sqrt{M}} \right) \sqrt{\mathcal{R}(\mathcal{X}_r, H_0)}.$$

Proof. See Appendix C.2. □

Theorems 3.1 and 3.2 reveal that the sample size M does not need to be large in practice, as the error $D_{(\cdot)}(\varphi_s^M, \pi)$ is dominated by the projection residual $\mathcal{R}(\mathcal{X}_r, H_0)$, which is independent of M .

4. Sample-based Gram matrix estimation

Given a subspace \mathcal{X}_r constructed from the matrix $H_k, k \in \{0, 1\}$, Sections 2 and 3 show that the approximation errors are bounded by $\mathcal{R}(\mathcal{X}_r, H_k)$. Since the gradient Gram matrix H_k has to be estimated through Monte Carlo integration in practice, here we provide rigorous estimates of how the sampling error of H_k affects the overall approximation error.

We start with a general importance sampling formulation for estimating the gradient Gram matrix. Suppose we can generate i.i.d. samples $X^i, i = 1, \dots, m$, from a density ν , then the Monte Carlo

estimators of H_0 and H_1 are given by

$$\begin{aligned}\widehat{H}_0 &= \frac{1}{m} \sum_{i=1}^m \nabla \log f(X^i) \nabla \log f(X^i)^\top \frac{\mu(X^i)}{\nu(X^i)}, \\ \widehat{H}_1 &= \frac{1}{m} \sum_{i=1}^m \nabla \log f(X^i) \nabla \log f(X^i)^\top \frac{\pi(X^i)}{\nu(X^i)}.\end{aligned}\tag{14}$$

For some function $h^m(X^1, \dots, X^m)$ where $X^i \sim \nu(x)$ are i.i.d. samples, we denote the expectation of h^m over all sampling outcomes of $X^i, i = 1, \dots, m$ by

$$\mathbb{E}_\nu[h^m] = \int \cdots \int h(x^1, \dots, x^m) \left(\prod_{i=1}^m \nu(x^i) \right) dx^1 \cdots dx^m.$$

For example, we have $\mathbb{E}_\nu[\widehat{H}_k] = H_k$. We also define the one-sample variance of the matrix estimators under the Frobenius norm $\|\cdot\|_F$ by

$$V(H_0, \nu) := \sum_{i,j=1}^d \text{var}_{X \sim \nu} \left[\partial_i \log f(X) \partial_j \log f(X) \frac{\mu(X)}{\nu(X)} \right] = m \mathbb{E}_\nu \left[\|\widehat{H}_0 - H_0\|_F^2 \right], \tag{15}$$

$$V(H_1, \nu) := \sum_{i,j=1}^d \text{var}_{X \sim \nu} \left[\partial_i \log f(X) \partial_j \log f(X) \frac{\pi(X)}{\nu(X)} \right] = m \mathbb{E}_\nu \left[\|\widehat{H}_1 - H_1\|_F^2 \right]. \tag{16}$$

Recall that in the LIS procedure, the reduced subspace \mathcal{X}_r is obtained as the d_r dimensional leading eigensubspace of H_k . The associated residual is given by $\mathcal{R}(\mathcal{X}_r, H_k) = \sum_{i=d_r+1}^d \lambda_i(H_k)$. In practice, we can only obtain the leading eigensubspace $\widehat{\mathcal{X}}_r$ generated by the sample-averaged matrix \widehat{H}_k . Thus, we must consider alternative residuals based on $\widehat{\mathcal{X}}_r$ and \widehat{H}_k . We first consider the ‘‘effective’’ residual $\mathcal{R}(\widehat{\mathcal{X}}_r, H_k)$, which provides upper bounds on the approximation errors induced by the estimated subspace $\widehat{\mathcal{X}}_r$, as given in Table 1. Note that the true matrix H_k must be used here. We aim to compare the residual $\mathcal{R}(\widehat{\mathcal{X}}_r, H_k)$ to the residual $\mathcal{R}(\mathcal{X}_r, H_k)$ to understand the impact of the sample-based estimation of the subspace \mathcal{X}_r . Since we cannot compute the effective residual $\mathcal{R}(\widehat{\mathcal{X}}_r, H_k)$ in practice, we must use the computable residual $\mathcal{R}(\widehat{\mathcal{X}}_r, \widehat{H}_k) = \sum_{i=d_r+1}^d \lambda_i(\widehat{H}_k)$ to determine the truncation dimension d_r . Thus, we also aim to estimate the difference between $\mathcal{R}(\widehat{\mathcal{X}}_r, H_k)$ and $\mathcal{R}(\widehat{\mathcal{X}}_r, \widehat{H}_k)$ to understand the reliability of the computable residual $\mathcal{R}(\widehat{\mathcal{X}}_r, \widehat{H}_k)$. The following variation of the Davis–Kahan Theorem [64] is useful for addressing these questions.

Lemma 4.1. *Let $\Sigma \in \mathbb{R}^{d \times d}$ and $\widehat{\Sigma} \in \mathbb{R}^{d \times d}$ be two positive semidefinite matrices. Let $\widehat{\mathcal{X}}_r$ be the d_r -dimensional leading eigensubspace of $\widehat{\Sigma}$ and \widehat{P}_\perp be the orthogonal projection to its complementary subspace. Then the following hold:*

- 1) $\mathcal{R}(\widehat{\mathcal{X}}_r, \Sigma) = \widehat{P}_\perp \Sigma \widehat{P}_\perp \leq \sum_{i=d_r+1}^d \lambda_i(\Sigma) + 2\sqrt{d_r} \|\widehat{\Sigma} - \Sigma\|_F$.
- 2) $\mathcal{R}(\widehat{\mathcal{X}}_r, \Sigma) = \widehat{P}_\perp \Sigma \widehat{P}_\perp \leq \sum_{i=d_r+1}^d \lambda_i(\widehat{\Sigma}) + \sqrt{d_r} \|\widehat{\Sigma} - \Sigma\|_F + \text{tr}(\Sigma - \widehat{\Sigma})$.

Proof. See Appendix D.1. □

A unique feature of these bounds is that they do not depend on eigenvalue gaps, which are usually necessary for finding the subspace correctly. Further implications will be discussed in Remark 4.4.

Theorem 4.2. *Under Assumption 2.1, suppose $\widehat{H}_k, k \in \{0, 1\}$ is computed by (14) and the computed subspace $\widehat{\mathcal{X}}_r$ is spanned by the d_r leading eigenvectors of \widehat{H}_k and the true subspace \mathcal{X}_r is spanned by the d_r leading eigenvectors of true H_k . Then the following bounds hold:*

- 1) *The effective residual satisfies $\mathbb{E}_\nu \left[\mathcal{R}(\widehat{\mathcal{X}}_r, H_k) \right] - \mathcal{R}(\mathcal{X}_r, H_k) \leq \frac{2}{\sqrt{m}} \sqrt{d_r V(H_k, \nu)}$.*
- 2) *The computable residual satisfies: $\mathbb{E}_\nu \left[\mathcal{R}(\widehat{\mathcal{X}}_r, H_k) - \mathcal{R}(\widehat{\mathcal{X}}_r, \widehat{H}_k) \right] \leq \frac{1}{\sqrt{m}} \sqrt{d_r V(H_k, \nu)}$.*

Proof. Using claim 1) of Lemma 4.1 and the identity

$$\mathbb{E}_\nu[\|H_k - \widehat{H}_k\|_F] \leq \sqrt{\mathbb{E}_\nu[\|H_k - \widehat{H}_k\|_F^2]} = \frac{\sqrt{d_r V(H_k, \nu)}}{\sqrt{m}},$$

claim 1) directly follows. Using the fact that $\mathbb{E}_\nu[\widehat{H}_k] = H_k$, $\mathbb{E}_\nu[\text{tr}(\widehat{H}_k - H_k)] = 0$, claim 2) follows from claim 2) of Lemma 4.1. \square

Claim 1) of Theorem 4.2 shows that the difference between the expected effective approximation residual using the sample average defined in (14) and the true approximation residual is of order $1/\sqrt{m}$, where the prefactor is controlled by the variance $V(H_k, \nu)$ and the dimension d_r . This reveals that, with increasing m , the approximation accuracy of the subspace given by the sample averages becomes closer to that of the true subspace. Claim 2) of Theorem 4.2 shows that the computable residual $\mathcal{R}(\widehat{\mathcal{X}}_r, \widehat{H}_k) = \sum_{i=d_r+1}^d \lambda_i(\widehat{H}_k)$ provides a reliable estimate of the approximation residual in expectation, where the reliability is controlled by the sample size m , the variance $V(H_k, \nu)$ and the subspace dimension d_r .

In the following corollary, we combine Theorem 4.2 with the results in Section 2 to address a practical problem: given the estimated $\widehat{H}_k, k \in \{0, 1\}$, quantify the associate LIS approximation error for estimating $\mathbb{E}_\pi[h]$. We use $\widehat{\varphi}_s(x), s \in \{f, g, l\}$, to denote the approximate target densities defined by an estimated subspace $\widehat{\mathcal{X}}_r$. Similar upper bounds for the statistical divergences discussed in Section 2 can also be established. We do not present them for the sake of conciseness.

Corollary 4.3. *For any bounded test function h , the estimation errors satisfy the following bounds:*

- 1) *Given $\widehat{\mathcal{X}}_r$ obtained from \widehat{H}_1 the resulting approximate target densities $\widehat{\varphi}_s, s \in \{f, g\}$, satisfy*

$$\begin{aligned} \mathbb{E}_\nu[\mathcal{E}_h(\pi, \widehat{\varphi}_s)] &\leq \kappa^{\frac{1}{2}} \left(\frac{\mathbb{E}_\pi[h^2] + \mathbb{E}_\nu[\mathbb{E}_{\widehat{\varphi}_s}[h^2]]}{2} \right)^{\frac{1}{2}} \left(\mathcal{R}(\mathcal{X}_r, H_1) + \frac{2\sqrt{d_r V(H_1, \nu)}}{\sqrt{m}} \right)^{\frac{1}{2}}, \\ \mathbb{E}_\nu[\mathcal{E}_h(\pi, \widehat{\varphi}_s)] &\leq \kappa^{\frac{1}{2}} \left(\frac{\mathbb{E}_\pi[h^2] + \mathbb{E}_\nu[\mathbb{E}_{\widehat{\varphi}_s}[h^2]]}{2} \right)^{\frac{1}{2}} \left(\mathbb{E}_\nu \left[\sum_{i=d_r+1}^d \lambda_i(\widehat{H}_1) \right] + \frac{\sqrt{d_r V(H_1, \nu)}}{\sqrt{m}} \right)^{\frac{1}{2}}. \end{aligned}$$

- 2) *Given $\widehat{\mathcal{X}}_r$ obtained from \widehat{H}_0 , the resulting approximate target density $\widehat{\varphi}_l$ satisfies*

$$\begin{aligned} \mathbb{E}_\nu[\mathcal{E}_h(\pi, \widehat{\varphi}_l)] &\leq \kappa^{\frac{1}{4}} \left(\frac{\|f\|_{2, \mu} (\mathbb{E}_\pi[h^2] + \mathbb{E}_\nu[\mathbb{E}_{\widehat{\varphi}_l}[h^2]])}{Z} \right)^{\frac{1}{2}} \left(\mathcal{R}(\mathcal{X}_r, H_0) + \frac{2\sqrt{d_r V(H_0, \nu)}}{\sqrt{m}} \right)^{\frac{1}{4}}, \\ \mathbb{E}_\nu[\mathcal{E}_h(\pi, \widehat{\varphi}_l)] &\leq \kappa^{\frac{1}{4}} \left(\frac{\|f\|_{2, \mu} (\mathbb{E}_\pi[h^2] + \mathbb{E}_\nu[\mathbb{E}_{\widehat{\varphi}_l}[h^2]])}{Z} \right)^{\frac{1}{2}} \left(\mathbb{E}_\nu \left[\sum_{i=d_r+1}^d \lambda_i(\widehat{H}_0) \right] + \frac{\sqrt{d_r V(H_0, \nu)}}{\sqrt{m}} \right)^{\frac{1}{4}}. \end{aligned}$$

Proof. For claim 1), recall that Theorem 2.4 applies to any given subspace, including $\widehat{\mathcal{X}}_r$, so we have

$$\mathbb{E}_\nu[\mathcal{E}_h(\pi, \hat{\varphi}_s)] \leq \sqrt{\frac{\kappa}{2} (\mathbb{E}_\pi[h^2] + \mathbb{E}_\nu[\mathbb{E}_{\hat{\varphi}_s}[h^2]])} \mathbb{E}_\nu[\mathcal{R}(\widehat{\mathcal{X}}_r, H_1)],$$

by the Cauchy–Schwarz inequality. Then we apply the upper bound of $\mathbb{E}_\nu[\mathcal{R}(\widehat{\mathcal{X}}_r, H_1)]$ in Theorem 4.2 to obtain the corollary. Claim 2) can be shown similarly. \square

Remark 4.4. *It is worth pointing out that our results did not discuss the difference between the estimated subspace $\widehat{\mathcal{X}}_r$ and the subspace \mathcal{X}_r obtained from the true H_k . (For a mathematical definition of this difference, one can refer to Theorem 1 in [64]). While finding the difference is possible using tools like the Davis–Kahan theorem, this difference is usually inversely proportional to the eigenvalue gap, i.e., $O(\lambda_1(H_k)/(\lambda_{d_r}(H_k) - \lambda_{d_r+1}(H_k)))$. See Theorem 1 in [64] for example. This quantity can be very large if the matrix H_k does not have a significant eigenvalue gap near the truncation dimension d_r . This is often observed in various applications, e.g., [17, 18, 30, 33], where eigenvalues of H_k decay rapidly. For example, if $\lambda_m(H_k) = m^{-2}$, then $(\lambda_{d_r}(H_k) - \lambda_{d_r+1}(H_k))^{-1} = O(d_r^3)$. For the numerical examples in Section 7, we observe that the eigenvalue gap is in the order of 10^{-4} to 10^{-5} for a moderate d_r . In other words, it is impractical to recover the subspace exactly.*

Fortunately, different eigenvectors of $\widehat{\mathcal{X}}_r$ have very different impact on the resulting approximate target density $\hat{\varphi}_s$. Intuitively, the accuracy of $\hat{\varphi}_s$ has little dependence on eigenvectors of H_k with close-to-zero eigenvalues, because they contribute little to H_k . But having accurate estimations for these eigenvectors is the most difficult, since their eigenvalues are close to each other. Our analysis avoids considering the difference between $\widehat{\mathcal{X}}_r$ and \mathcal{X}_r and focuses on the difference between π and $\hat{\varphi}_s$, since the latter does not need the eigenvalue gap and is the purpose of identifying the subspace.

In importance sampling, the proposal density ν plays an important role in the sampling accuracy. In particular, the one-sample importance sampling variance of the Gram matrix can be bounded by the likelihood ratio between ν and μ , or ν and π , as follows.

Proposition 4.5. *We have the following upper bounds for the sampling variance of the Gram matrix*

$$V(H_0, \nu) \leq \mathbb{E}_{X \sim \nu} \left[\|\nabla \log f(X)\|^4 \frac{\mu(X)^2}{\nu(X)^2} \right], \quad V(H_1, \nu) \leq \mathbb{E}_{X \sim \nu} \left[\|\nabla \log f(X)\|^4 \frac{\pi(X)^2}{\nu(X)^2} \right].$$

Proof. See Appendix D.2. \square

Proposition 4.5 shows that one should make the ratios, $\frac{\mu}{\nu}$ and $\frac{\pi}{\nu}$, close to one in order to minimize the sampling variance for H_0 and H_1 , respectively. For estimating H_0 , we can naturally use the reference distribution, which is easy to sample from, as the biasing distribution, i.e., $\nu = \mu$. For estimating H_1 , the second inequality in Proposition 4.5 suggests that using the reference distribution may not be a feasible strategy. Consider a scenario where the likelihood function is bounded as $\sup_x f = 1$ and the gradient of the log-likelihood is bounded as $\sup_x \|\nabla \log f(x)\| = M_f$. Using $\nu = \mu$, the variance $V(H_1, \mu)$ is inversely quadratic in the normalizing constant Z , i.e., $V(H_1, \mu) \leq M_f^4 / Z^2$. For a target density concentrating in a small region of the parameter space, the normalizing constant Z can take a small value, and thus the variance $V(H_1, \mu)$ can take a rather large value. This way, alternative strategies such as MCMC and SMC must be used to adaptively collect samples from the target distribution for estimating H_1 , while the intermediate estimation of H_1 provides approximate target densities that can be used to accelerate MCMC and SMC. Further details are presented in the next section.

5. Integration with MCMC and SMC

In this section, we discuss the integration of MCMC and SMC with the approximate target densities defined by LIS for estimating the Gram matrix H_1 .

5.1. MCMC with LIS

For a given target density $\pi(x)$, the Metropolis–Hastings (MH) method employs a proposal density $p(x, x')$ and an acceptance/rejection step with the acceptance probability

$$\beta(x, x') = 1 \wedge \frac{\pi(x')p(x', x)}{\pi(x)p(x, x')}$$

to construct a Markov chain of random variables with $\pi(x)$ as the invariant density. With the subspace identified by the LIS approach, we can apply different strategies to different subspaces to accelerate the convergence of MCMC. For a given subspace \mathcal{X}_r , we can formulate an MCMC transition kernel on \mathcal{X}_r that has one of the lower-dimensional surrogate densities $\bar{\varphi}_s(x_r)$, $s \in \{f, g, l\}$, as the invariant density. Then, combining the transition kernel on \mathcal{X}_r and the conditional reference density $\mu(x_\perp | x_r)$, we can define a Markov chain transition kernel that has the full target density $\pi(x)$ as the invariant density. This procedure is summarized in Algorithm 1.

Algorithm 1: MCMC with LIS proposal

Input: target density $\pi(x)$, an initial state $X^0 = x^0$, a LIS subspace \mathcal{X}_r , proposal density p , conditional reference density $\mu(\cdot | \cdot)$, likelihood function f , and lower-dimensional surrogate density $\bar{\varphi}_s$, $s \in \{f, g, l\}$, iteration count t

Output: a Markov chain X^1, \dots, X^t

- 1 **for** $j = 1, \dots, t$ **do**
 - 2 Given the previous state $X^{(j-1)} = x$, decompose it as $x = x_r + x_\perp$ based on the subspace decomposition $\mathbb{R}^d = \mathcal{X}_r \oplus \mathcal{X}_\perp$;
 - 3 Generate a MCMC proposal $x'_r \sim p(x_r, \cdot)$;
 - 4 Let $x'_r = x_r$ with rejection probability $1 - \beta(x_r, x'_r)$, $\beta(x_r, x'_r) = 1 \wedge \frac{\bar{\varphi}_s(x'_r)p(x'_r, x_r)}{\bar{\varphi}_s(x_r)p(x_r, x'_r)}$;
 - 5 Generate a proposal $x'_\perp \sim \mu(x_\perp | x_r)$ and set $x' = x'_r + x'_\perp$;
 - 6 Compute the acceptance probability $\alpha(x, x') = 1 \wedge \frac{f(x')\bar{\varphi}_s(x_r)\bar{\mu}(x'_r)}{f(x)\bar{\varphi}_s(x_r)\bar{\mu}(x_r)}$;
 - 7 With probability $\alpha(x, x')$, accept the complement proposal and set $X^j = x'$, otherwise reject x' and set $X^j = x$.
-

The acceptance and rejection steps used in lines 4 and 7 of Algorithm 1 are consistent with the approximation of the target density. Since the lower-dimensional surrogate density $\bar{\varphi}_s(x_r)$ carries most of the information provided by the likelihood function, it may have a complicated structure to explore. However, the rather low dimensionality of $\bar{\varphi}_s(x_r)$ makes it possible to design efficient MCMC transition kernels. Note that the product of the lower-dimensional surrogate density and the conditional reference density, $\bar{\varphi}_s(x_r)\mu(x_\perp | x_r)$, defines an approximation of the full-dimensional target density, in which the approximation accuracy has been extensively analyzed in previous sections. This way, in the complement space \mathcal{X}_\perp , we embed $\mu(x_\perp | x_r)$, which is an approximation of $\pi(x_\perp | x_r)$, into another MCMC transition kernel to explore the full-dimensional target density $\pi(x)$. Thus, the efficiency of the complement subspace MCMC transition in lines 5–7 of Algorithm 1 should strongly depend on

its acceptance rate. In the following proposition, we show that $\pi(x)$ is indeed the invariant measure of Algorithm 1. In addition, we also provide a lower bound on the complement transition acceptance rate in line 6 of Algorithm 1.

Proposition 5.1. *The full-dimensional target density $\pi(x)$ is the invariant density for Algorithm 1. Moreover, the expected acceptance rate for the x_\perp part is lower bounded by*

$$\mathbb{E} [\alpha(X, X')] \geq 1 - 4\sqrt{2}D_H(\pi, \varphi_s).$$

Here X is a random sample from π and X' is a proposal generated by Algorithm 1.

Proof. See Appendix E.1. □

Proposition 5.1 indicates that when running Algorithm 1, the acceptance rate of the MCMC transition in the complement subspace \mathcal{X}_\perp is controlled by the accuracy of the approximate target density. One anticipates that the acceptance rate in line 6 approaches 1 if the approximation error approaches 0. In other words, the efficiency of Algorithm 1 depends largely on the efficiency of the MCMC on the low dimensional \mathcal{X}_r . To implement Algorithm 1, we need the lower-dimensional surrogate density $\bar{\varphi}_s, s \in \{f, g, l\}$. This in practice can be replaced by the Monte Carlo version $\bar{\varphi}_s^M$ (cf. Definitions 1.1–1.3), with accuracy guaranteed by Theorems 3.1 and 3.2. Note that the surrogate density $\bar{\varphi}_f^M(x_r)$ provides an unbiased estimate of the marginal target density $\bar{\pi}(x_r)$. In [24], this is used together with the pseudo-marginal technique [4, 5] to design alternative sampling methods.

Another key ingredient in Algorithm 1 is the LIS subspace \mathcal{X}_r , which is obtained by estimating either the matrix H_0 or the matrix H_1 . While H_0 is easy to compute, the resulting subspace may have inferior approximation accuracy compared with that obtained by H_1 . However the estimation of H_1 often requires samples from the target $\pi(x)$ (cf. Section 4). To resolve this dilemma, we consider to adaptively estimate H_1 and the LIS \mathcal{X}_r within MCMC. The procedure is summarized in Algorithm 2.

Algorithm 2: MCMC with adaptive LIS

Input: target density $\pi(x)$, reference density μ , likelihood function f , number of epochs K , iteration count t , and a truncation index K_*

Output: a Markov chain $X^1, \dots, X^{(K+1)t}$ and a subspace \mathcal{X}_r

- 1 Generate X^1, \dots, X^t from μ and compute $H^{(0)} = \frac{1}{t} \sum_{i=1}^t \nabla \log f(X^i) \nabla \log f(X^i)^\top$;
 - 2 Find the leading eigenvectors $\{v_1, \dots, v_{d_r}\}$ of $H^{(0)}$ to define $\mathcal{X}_r = \text{span}\{v_1, \dots, v_{d_r}\}$;
 - 3 **for** $j = 1, \dots, K$ **do**
 - 4 Run Algorithm 1 with target density π , initial state X^{jt} , and LIS subspace \mathcal{X}_r for t iterations to generate the Markov chain $X^{jt+1}, \dots, X^{j(t+t)}$;
 - 5 Compute $H^{(j)} = \frac{1}{t} \sum_{i=1}^t \nabla \log f(X^{jt+i}) \nabla \log f(X^{jt+i})^\top$;
 - 6 Compute $\bar{H} = \frac{1}{j+1 - \min(j, K_*)} \sum_{i=\min(j, K_*)}^j H^{(i)}$;
 - 7 Find the leading eigenvectors $\{v_1, \dots, v_{d_r}\}$ of \bar{H} to define $\mathcal{X}_r = \text{span}\{v_1, \dots, v_{d_r}\}$;
-

Our starting point is an initial LIS \mathcal{X}_0 that can be estimated using H_0 . Then, we run Algorithm 1 using \mathcal{X}_0 to generate samples from π . We call this the first epoch. Algorithm 1 in this epoch might not be efficient, since \mathcal{X}_0 may not be a good subspace. However, we can re-estimate the matrix H_1 and an improved LIS \mathcal{X}_1 using the samples in the first epoch. Then, the updated \mathcal{X}_1 is used in the next epoch to run Algorithm 1. This procedure can be carried out iteratively, where each epoch creates better estimates of the Gram matrix H_1 and the corresponding LIS. The truncation index K_* is introduced

to discard burn-in samples from initial epochs in estimating H_1 . Since the subspace estimation error follows a Monte Carlo convergence rate (cf. Theorem 4.2), we often only need to implement Algorithm 2 for $O(10^3)$ iterations in each epoch to estimate the LIS \mathcal{X}_r in many practical scenarios. In practice, the LIS usually stabilizes after a few epochs (e.g., about 10 epochs) of training, so in total $O(10^4)$ iterations are needed to build the LIS. Then, the estimated subspace \mathcal{X}_r can be used in the non-adaptive Algorithm 1 to explore the target density.

5.2. SMC with LIS

For target densities with complicated and multi-modal structures, SMC offers an efficient alternative to MCMC. Here we present the integration of SMC with LIS. This integration also offers a layered subspace construction procedure that is naturally embedded within SMC. In our context, SMC uses a sequence of densities $\pi_k, k \in 0, \dots, K$, such that $\pi_0 = \mu, \pi_K = \pi$, and each ratio π_{k+1}/π_k has a small variance. For example, one can obtain such a sequence using the tempering formula

$$\pi_k(x) = \frac{1}{Z_k} \mu(x) f(x)^{\beta_k}, \quad Z_k = \int \mu(x) f(x)^{\beta_k} dx, \quad k \in 0, 1, \dots, K,$$

where $\beta_k \geq 0$ is an increasing sequence with $\beta_0 = 0$ and $\beta_K = 1$. This way, given samples from π_k , one can apply importance sampling to obtain weighted samples from π_{k+1} and estimate associated statistics. Then, these statistics can be used to formulate MCMC transition kernels with the invariant density π_{k+1} to update the weighted samples. This procedure is summarized in Algorithm 3.

Algorithm 3: SMC for LIS proposal

Input: likelihood function f , reference density μ , tempering coefficients β_k and iteration count t_k for each level $k \in 1, \dots, K$
Output: Samples X^1, \dots, X^T from $\pi \propto f\mu$

- 1 Generate samples X^1, \dots, X^T from $\pi_0 = \mu$;
- 2 **for** $k \in 0, \dots, K - 1$ **do**
- 3 Compute the weights $W^j = f^{\beta_{k+1} - \beta_k}(X^j)$ for $j = 1, \dots, T$;
- 4 Let $H'_1 = (\sum_{j=1}^T W^j)^{-1} \sum_{j=1}^T \nabla \log f(X^j) \nabla \log f(X^j)^\top W^j$;
- 5 Find the leading eigenvectors $\{v_1, \dots, v_{d_r}\}$ of H'_1 to define $\mathcal{X}_r = \text{span}\{v_1, \dots, v_{d_r}\}$;
- 6 **for** $t = 1, \dots, T$ **do**
- 7 Draw a resampling index J from the categorical distribution with the probability mass function $\mathbb{P}[J = j] \propto W^j, j = 1, \dots, T$, and set $Y^0 = X^J$;
- 8 Run MCMC Algorithm 1 with the invariant density $\pi_{k+1} \propto \mu f^{\beta_{k+1}}$, initial state Y^0 , LIS subspace \mathcal{X}_r , iteration count t_k , let Y^1, \dots, Y^{t_k} be the output ;
- 9 Update $X^t = Y^{t_k}$;

In Algorithm 3, a resampling step is used to transform a weighted particle representation of π_{k+1} into an equally weighted particle representation, followed by MCMC updates. In practice, the tempering coefficients can be chosen adaptively. Given the weighting function $f^{\beta_{k+1} - \beta_k}(x)$, one can choose the next tempering coefficient β_{k+1} such that

$$\frac{\mathbb{E}_{\pi_k} \left[f^{\beta_{k+1} - \beta_k}(X) \right]^2}{\mathbb{E}_{\pi_k} \left[f^{\beta_{k+1} - \beta_k}(X)^2 \right]} \approx \frac{ESS}{n} < \tau, \quad \text{where } ESS = \frac{\left(\sum_{i=1}^n f^{\beta_{k+1} - \beta_k}(X^i) \right)^2}{\sum_{i=1}^n f^{\beta_{k+1} - \beta_k}(X^i)^2}$$

is the effective sample size and $\tau \in (0, 1)$ is a predetermined threshold.

For each tempering coefficient β_{k+1} , we construct the matrix H_1 for the corresponding target density π_{k+1} using importance sampling with π_k as the importance density, and then build MCMC transition kernels as described in Algorithm 1. Denoting the matrix H_1 for the density π_{k+1} by $H_1^{(k+1)}$, its importance sampling estimate takes the form $\mathbb{E}_{\pi_k}[H^{(k,k+1)}(X)]$, where

$$H^{(k,k+1)}(x) = \frac{Z_k}{Z_{k+1}} \nabla \log f(x) \nabla \log f(x)^\top f(x)^{(\beta_{k+1} - \beta_k)}.$$

The introduction of the tempering sequence reduces the variance of each H_1 estimation compared to the direct estimation of H_1 from the reference μ . This can be characterized in the following proposition.

Proposition 5.2. *Suppose $\|\nabla \log f(x)\|^4 f(x)^{\beta_{k+1} + \delta}$ with $\delta = \beta_{k+1} - \beta_k$ is integrable under the reference μ . Then the variance upper bound*

$$V_{k+1}(H_1, \pi_k) := \sum_{i,j=1}^d \text{var}_{X \sim \pi_k} \left[[H^{(k,k+1)}(X)]_{ij} \right] \leq \frac{Z_k}{Z_{k+1}} \mathbb{E}_{\pi_{k+1}} \left[\|\nabla \log f(X)\|^4 f(X)^\delta \right]$$

for the subspace estimation in SMC is finite.

Proof. See Appendix E.2. □

By setting $\nu = \mu$ in the inequality for $V(H_1, \nu)$ in Proposition 4.5, and by using that $\pi(x)/\mu(x) = \frac{1}{Z} f(x)$ for a.e. x , it follows that $V(H_1, \mu)$ is finite if $\|\nabla \log f(x)\|^4 f(x)^2$ is integrable with respect to μ . This is strictly stronger than the requirement in Proposition 5.2 if and only if $\beta_{k+1} + \delta < 2$. The latter condition is valid as soon as $K \geq 2$ tempering coefficients are used. Consider the same example used in Section 4 where the likelihood function is bounded as $\sup_x f = 1$ and the gradient of the log-likelihood is bounded as $\sup_x \|\nabla \log f(x)\| = M_f$. The variance $V_{k+1}(H_1, \pi_k)$ in SMC satisfies

$$V_{k+1}(H_1, \pi_k) \leq \frac{M_f^4 Z_k}{Z_{k+1}},$$

which can be much smaller than the upper bound $V(H_1, \mu) \leq M_f^4 / Z^2$ of the direct importance sampling formula in Proposition 4.5. On the other hand, one needs to implement the SMC scheme which is in general more involved and computationally more expensive than using importance sampling.

6. Dimension independent errors for linear inverse problems

LIS mainly targets high-dimensional problems with intrinsic low-dimensional structures. For infinite-dimensional problems, it is highly desired that the subspace approximation error (e.g., the result in Corollary 4.3) is independent of the ambient parameter dimension d . While the dimension independence of sampling methods has been extensively investigated in the literature, see [20] and references therein, there has been little investigation on the dimension independence of LIS. Intuitively, for the approximation error to be dimension independent, $H_k, k \in \{0, 1\}$ must be trace-class in the limit as $d \rightarrow \infty$ and the variance $V(H_k, \nu)$ must be bounded independently of d . It is an open question to establish conditions under which these properties hold for general likelihood functions. We will show

that the two conditions above are satisfied for linear Gaussian Bayesian inverse problems, i.e. where the prior and likelihood are Gaussian and the parameter-to-observable map is linear.

We consider a Bayesian problem with unknown parameter $z \in \mathbb{R}^d$ and the prior $p_0(z)$ being $\mathcal{N}(0, \Gamma)$. Given a linear parameter-to-observable map G , the data are given by

$$Y = GZ + \xi, \quad \xi \sim \mathcal{N}(0, I_{d_y}).$$

Applying a whitening transformation $X = \Gamma^{-1/2}Z$, we obtain $X \sim \mu(x)$ where $\mu(x) = \mathcal{N}(0, I_d)$ and

$$Y = AX + \xi, \quad A = G\Gamma^{1/2}.$$

This defines the likelihood function $f(x) = \exp(-\frac{1}{2}\|Ax - Y\|^2)$. First we will establish a series of estimates for the quantities we derived in previous sections.

Proposition 6.1. *Denote $C_A = A^\top A = G^\top \Gamma G$. The following hold:*

- 1) *The eigenvalues of H_0 are controlled by $\lambda_{i+1}(H_0) \leq \lambda_i(C_A)^2$.*
- 2) *The eigenvalues of H_1 are controlled by $\lambda_{i+1}(H_1) \leq \lambda_i(C_A)^2 / 1 + \lambda_i(C_A)$.*
- 3) *The normalizing constant is bounded by $\sqrt{\det(C_A + I)} \leq \frac{1}{Z} \leq \sqrt{\det(C_A + I)} \exp(\frac{1}{2}\|y\|^2)$.*
- 4) *The constant $\frac{\|f\|_{2,\mu}}{Z}$ is bounded by $\frac{\|f\|_{2,\mu}}{Z} \leq \det(I + C_A^2)^{1/4} \exp(\frac{1}{2}(\sqrt{2} - 1)^2\|y\|^2)$*
- 5) *When the reference density μ is used for estimating $H_k, k \in \{0, 1\}$, the variances are bounded by*

$$V(H_0, \mu) \leq 6 \left(\left(\sum_{i=1}^d \lambda_i(C_A)^2 \right)^2 + \|A^\top y\|^4 \right),$$

$$V(H_1, \mu) \leq 6 \sqrt{\det(I + C_A^2)} \exp\left((\sqrt{2} - 1)^2\|y\|^2\right) \left(\left(\sum_{i=1}^d \frac{\lambda_i(C_A)^2}{1 + 2\lambda_i(C_A)} \right)^2 + \|A^\top y\|^4 \right).$$

- 6) *The SMC sampling variance in Proposition 5.2 is bounded by*

$$V_{k+1}(H_1, \pi_k) \leq 6 \sqrt{\det(I + \delta^2 C_A^2)} \exp\left(\delta^2 \|A^\top y\|^2\right) \left(\left(\sum_{i=1}^d \frac{\lambda_i(C_A)^2}{1 + \tau \lambda_i(C_A)} \right)^2 + \|A^\top y\|^4 \right).$$

where $\delta = \beta_{k+1} - \beta_k$ and $\tau = \beta_{k+1} + \delta$.

Proof. See Appendix F.1. □

Claim 1) implies that the spectrum of H_0 is bounded by the spectrum of C_A^2 . Claim 2) implies that the spectrum of H_1 is bounded by the spectrum of $C_A^2(I + C_A)^{-1}$. Note that

$$\frac{\lambda_i(C_A)^2}{1 + \lambda_i(C_A)} \leq \lambda_i(C_A)^2,$$

and the ratio between the two is large if $\lambda_i(C_A)$ is large. Also recall that in Remark 2.5, we showed the approximation errors with subspace obtained from H_0 involve the pre-constant $1/Z$, which is estimated in claim 3), but not the subspace obtained from H_1 . Thus, in the Gaussian linear setting,

the error estimates obtained from H_1 will be much tighter than those obtained from H_0 when the dominating eigenvalues of C_A are large, which is often the case in practice.

On the other hand, H_0 is easier for Monte Carlo based estimations than H_1 . This can be seen from the bounds on the variance of the Gram matrices in claim 5). Comparing with $V(H_0, \mu)$, $V(H_1, \mu)$ has an additional dependence on $\det(I + C_A^2)$ and $\exp\left(\frac{1}{2}(\sqrt{2}-1)^2\|y\|^2\right)$. Claim 6) shows that this estimation difficulty can be remedied by SMC, because the upper bound of the variance $V_{k+1}(H_1, \pi_k)$ is smaller than that of $V(H_1, \mu)$.

In many applications, the spectrum of the prior covariance Γ is assumed to exhibit polynomial decay, i.e. $\lambda_j(\Gamma) \leq C_\Gamma j^{-\alpha}$, $\alpha > 0$. This kind of assumption is common for functional data analysis [18, 33, 50] and inverse problems [57]. With $\alpha > 1/2$, the prior covariance is trace-class, and thus the prior has measure 1 on some suitably constructed Banach space. In the following corollary, we replace the bounds in Proposition 6.1 with estimates obtained using this trace-class constraint to demonstrate the dimension scalability.

Corollary 6.2. *Suppose the eigenvalues of Γ exhibit polynomial decay, $\lambda_j(\Gamma) \leq C_\Gamma j^{-\alpha}$ with $\alpha > 1/2$, the observation matrix G has bounded ℓ^2 operator norm, and the observed data have bounded ℓ^2 norm. Then the following estimates hold independently of the ambient parameter dimension d . Consequently, the estimation error \mathcal{E}_h for any bounded h is independent of d by Corollary 4.3.*

1) When using \mathcal{X}_r as the subspace spanned by the first d_r eigenvectors of H_k , $k \in \{0, 1\}$,

$$\mathcal{R}(\mathcal{X}_r, H_k) \leq \frac{1}{2\alpha - 1} \|G\|^4 C_\Gamma^2 (d_r - 1)^{1-2\alpha}.$$

2) The constant $\frac{\|f\|_{2,\mu}}{Z}$ is bounded by $\frac{\|f\|_{2,\mu}}{Z} \leq \exp\left(\frac{1}{2}(\sqrt{2}-1)^2\|y\|^2 + \frac{\alpha}{4\alpha-2}\|G\|^4 C_\Gamma^2\right)$.

3) When the reference distribution μ is used for estimating the matrices H_k , $k \in \{0, 1\}$, the variances are bounded by

$$V(H_0, \mu) \leq 6 \left(\frac{4\alpha^2}{(2\alpha - 1)^2} \|G\|^8 C_\Gamma^4 + \|A^\top y\|^4 \right),$$

$$V(H_1, \mu) \leq 6 \exp\left((\sqrt{2}-1)^2\|y\|^2 + \frac{\alpha}{2\alpha-1}\|G\|^4 C_\Gamma^2 \right) \left(\frac{4\alpha^2}{(2\alpha-1)^2} \|G\|^8 C_\Gamma^4 + \|A^\top y\|^4 \right).$$

4) The SMC sampling variance in Proposition 5.2 is bounded by

$$V_{k+1}(H_1, \pi_k) \leq 6 \exp\left(\delta^2 \|A^\top y\|^2 + \frac{\delta^2 \alpha}{2\alpha-1} \|G\|^4 C_\Gamma^2 \right) \left(\frac{4\alpha^2}{(2\alpha-1)^2} \|G\|^8 C_\Gamma^4 + \|A^\top y\|^4 \right).$$

where $\delta = \beta_{k+1} - \beta_k$.

Proof. See Appendix F.2. □

7. Numerical examples

Now we provide several numerical examples to illustrate the theoretical results developed in the preceding sections. We start with a synthetic linear inverse problem to demonstrate various likelihood approximation methods and continue with a more practical nonlinear Bayesian inference problem governed by a partial differential equation (PDE).

7.1. Example 1: synthetic example

In the first example, we consider a Bayesian inverse problem with linear observations and log-normal prior. Problems of this type are applied in X-ray tomography and atmospheric remote sensing, see [32] and references therein. The parameter to be inferred can be modeled by a random Gaussian vector $X \sim \mu = \mathcal{N}(0, \Gamma)$, where $\Gamma \in \mathbb{R}^{d \times d}$ is the prior covariance matrix. The observation data are modeled through

$$Y = G \exp(X) + \xi, \quad \xi \sim \mathcal{N}(0, \sigma^2 I_{d_y}),$$

where $G \in \mathbb{R}^{d_y \times d}$ is a matrix. The observation likelihood is then given by

$$f(x; y) \propto \exp\left(-\frac{1}{2\sigma^2} \|y - G \exp(x)\|^2\right).$$

To compare different approximations by exploring regimes where the data have differing impacts on different parameter directions, we generate random observation matrices and prescribe the spectra of the observation matrix and the prior covariance matrix. We specify the prior covariance by setting $\Gamma = \text{diag}(\gamma_1, \gamma_2, \dots, \gamma_d)$ with $\gamma_j = \gamma_0 j^{-\beta_\gamma}$. To create a random observation matrix G , we use the reduced singular value decomposition $G = U \Lambda V^\top$, where the matrices U and V are randomly and independently generated from the orthogonal group [56] and $\Lambda = \text{diag}(\lambda_1, \lambda_2, \dots, \lambda_{d_y})$ with $\lambda_j = \lambda_0 j^{-\beta_\lambda}$. In particular, U and V are computed using a QR decomposition of a matrix of independent standard Gaussian entries. By using randomly generated G , we can confirm the observed phenomena are not restricted to a specific choice of G . In this example, we present 3 independently generated G , and we will see the numerical results have little differences among them. The problem dimensions are set to $d = 500$ and $d_y = 50$. The variables that determine Γ and G are given by $\gamma_0 = 4$, $\beta_\gamma = -2$, $\lambda_0 = 100$, and $\beta_\lambda = -1$. The standard deviation of the observation noise is given by $\sigma = 1$.

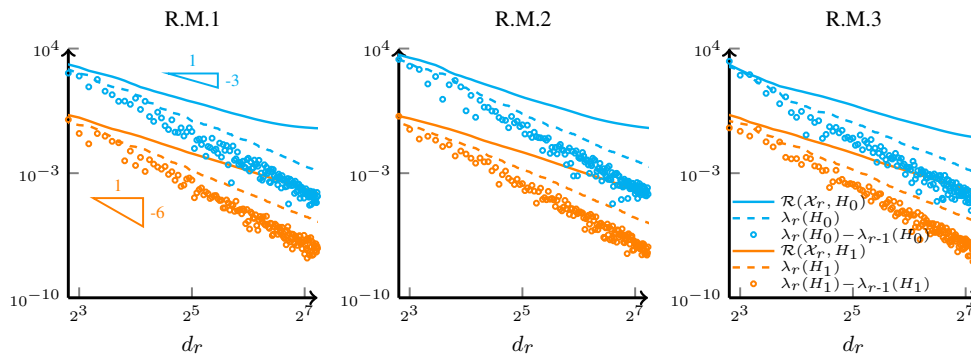


Figure 1. Synthetic example. Eigenvalues and the gaps of eigenvalues of H_k matrices for three randomly generated observation maps (R.M.) and the sums of the residual eigenvalues versus the projection dimensions.

We present the numerical results based on three realizations of the randomly generated G matrices. For each test case, we construct the “true” matrix H_0 using 5×10^5 Monte Carlo samples and construct the “true” matrix H_1 using 5×10^6 MCMC samples. As shown in Figure 1, for all three test cases, the eigenvalues of H_1 matrices are several orders smaller than those of H_0 matrices, and thus the sums

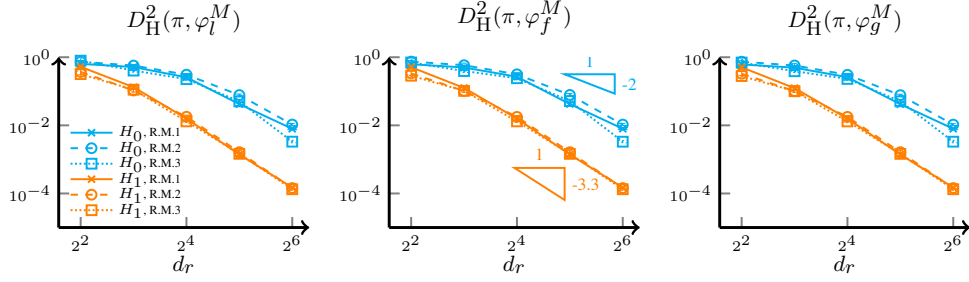


Figure 2. Synthetic example. Approximation errors of the approximate posterior densities versus projection dimensions for different H_k matrices and different approximation methods. From left to right, approximation methods are φ_l^M , φ_f^M , and φ_g^M , respectively. Sample size $M = 4$ is used in computing the conditional expectation.

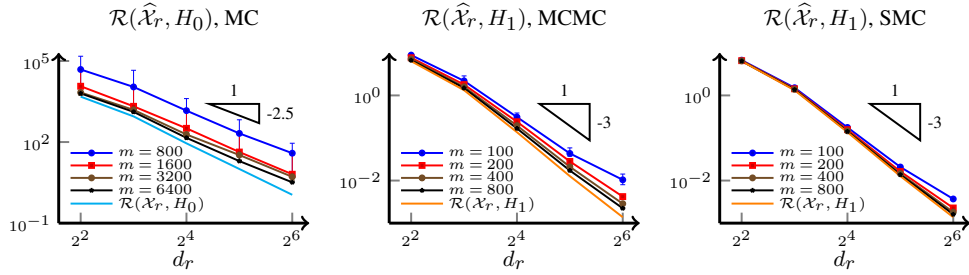


Figure 3. Synthetic example with the first random observation matrix. The sums of the residual eigenvalues versus projection dimensions for different H_k matrices and subspaces $\hat{\mathcal{X}}_r$ computed using different samples sizes m and different methods. From left to right, we have Monte Carlo estimation of \hat{H}_0 , MCMC estimation of \hat{H}_1 , and SMC estimation of \hat{H}_1 , respectively. The error bars represent [10%, 90%] quantiles estimated using 100 runs.

of the residual eigenvalues, $\mathcal{R}(\mathcal{X}_r, H_1)$, are significantly lower than $\mathcal{R}(\mathcal{X}_r, H_0)$. This suggests that the approximate posterior density induced by the H_1 matrix should have better accuracy compared with that defined by the H_0 matrix in this example. This is confirmed in Figure 2, which shows the squared Hellinger distances between the true posterior and three approximations φ_s^M , $s \in \{f, g, l\}$ introduced in Section 3. For all posterior approximation methods, the approximation subspaces defined by H_1 matrices yield significantly smaller squared Hellinger distances than those of H_0 matrices.

The eigenvalue gaps, $\lambda_r - \lambda_{r-1}$, are also plotted in Figure 1. Note that we use the same x-axis by assuming $r = d_r$. The eigenvalue gaps decay to zero quickly. In particular, for H_1 , the gap is around 10^{-3} for a moderate reduction dimension $r = 32$, and 10^{-7} for a larger dimension $r = 128$. For H_0 , the effective eigenvalue gaps are of similar values, since we need to divide it by λ_1 , which is around 10^4 for H_0 . This illustrates that it is important for the theoretical results to be independent of eigenvalue gaps, as explained in Remark 4.4.

Since all the numerical results are similar among all three randomly generated observation matrices, we will focus on the first realization for subsequent discussion. Next, we investigate the impact of sample size m for estimating the lower-dimensional subspace $\hat{\mathcal{X}}_r$. Figure 3 presents the quantiles of the sums of the residual errors for various sample-based subspace estimations. Although both H_0 and H_1 matrices have diminishing eigenvalue gaps in this example (c.f. Figure 1), the sample-based estimations still exhibit sufficient accuracy in probing the dimension reduced subspaces. For example, with a rather

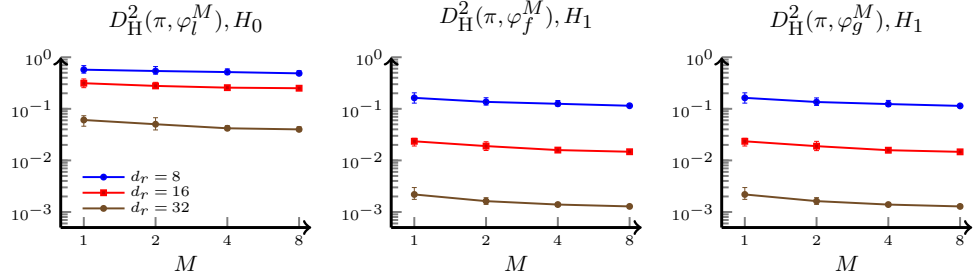


Figure 4. Synthetic example with the first random observation matrix. Approximation errors of the approximate posterior densities (with projection dimensions $d_r = \{8, 16, 32\}$) versus sample sizes $M = \{1, 2, 4, 8\}$. From left to right, approximation methods are φ_l^M with the matrix H_0 , φ_f^M with the matrix H_1 , and φ_g^M with the matrix H_1 , respectively. The error bars represent [10%, 90%] quantiles estimated using 100 runs.

small sample size $m = 100$, using either MCMC or SMC can lead to accurate subspace estimations for the approach based on the H_1 matrix. This confirms the findings of our analysis in Section 4. In addition, the SMC-based estimation has better accuracy compared to that of MCMC-based estimation, which is also anticipated by our analysis in Section 5.

Finally, we investigate the Monte Carlo sample size M for computing the conditional expectations in various approximate posteriors, as discussed in Section 3. The results presented in Figure 4 confirm the results of our analysis. For problems with rather small residual eigenvalues $\mathcal{R}(\mathcal{X}_r, H_k)$, a small sample size M is sufficient for accurate estimation of the conditional expectations. Increasing M only leads to a marginal improvement in the approximation accuracy in this example. The reasons behind this were explained at the end of Section 3.

7.2. Example 2: PDE problem

We consider a classical Bayesian inverse problem governed by an elliptic PDE [26, 28]. Such problems arise in subsurface flows and oil reservoir management. Fix a domain of interest D with boundary ∂D . The potential function $t \mapsto u(t)$ where $t \in D \subset \mathbb{R}^2$ is modeled by the PDE

$$-\nabla \cdot (\kappa(t) \nabla u(t)) = 0, \quad t \in D := (0, 1)^2, \quad (17)$$

with Dirichlet boundary conditions $u|_{t_1=0} = 1$ and $u|_{t_1=1} = 0$ on the left and right boundaries, and homogeneous Neumann conditions on other boundaries. The diffusion coefficient $\kappa(t)$ should be positive, and thus it is often parametrized by its logarithm, i.e., $\kappa(t) = \exp(x(t))$. The goal is to infer the unknown parameter function $x(t)$ from d_y incomplete observations of the potential function $u(t)$. Following the setup of [23], a zero-mean Gaussian process prior with the exponential kernel

$$K(t, t') = \exp\left(-\frac{1}{\ell} \|t - t'\|\right)$$

is prescribed to the unknown parameter $x(t)$.

Given an arbitrary function $x(t)$, the PDE (17) cannot be solved analytically. This way, the functions $x(t)$ and $u(t)$ need to be discretized to numerically solve (17). We tessellate the spatial domain D with a uniform triangular grid with mesh size h , and then define continuous, piecewise

quadratic finite element (FE) basis functions $\{\phi_1(t), \dots, \phi_d(t)\}$ with cardinality d . Then, the infinite dimensional functions $x(t)$ and $u(t)$ can be approximated by $x(t) \approx x_h(t) := \sum_{i=1}^d \phi_i(t)x_i$ and $u(t) \approx u_h(t) := \sum_{i=1}^d \phi_i(t)u_i$, respectively. After discretization, the unknown function $x_h(t)$ can be effectively represented by a coefficient vector $x = (x_1, \dots, x_d)$, which yields a multivariate Gaussian prior $\mu(x) := \mathcal{N}(0, \Gamma)$ where $\Gamma_{ij} = \int \int K(t, t') \phi_i(t) \phi_j(t') dt dt'$.

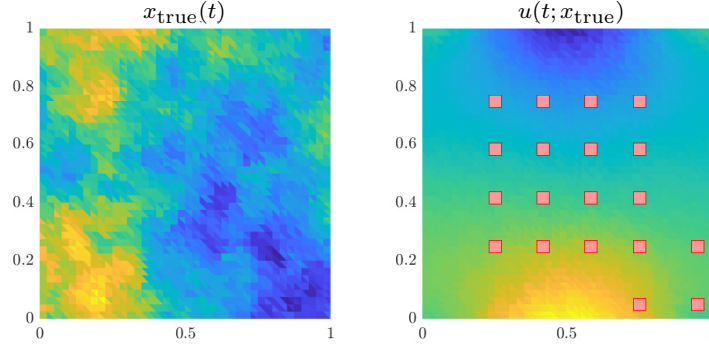


Figure 5. Setup of the PDE inverse problem. Left: the true parameter $x_{\text{true}}(t)$ used for generating synthetic data. Right: the corresponding potential function $u(t; x_{\text{true}})$ and observation locations.

For any given parameter coefficients x , the corresponding discretized potential function $u_h(t; x)$ is obtained by solving the Galerkin projection of the PDE (17). Observations are collected as $d_y = 19$ local averages of the potential function $u(t)$ over sub-domains $D_i \subset D$, $i = 1, \dots, d_y$. The subdomains are shown by the squares in Figure 5. To simulate the observable model outputs, we define the forward model $G : \mathbb{R}^d \mapsto \mathbb{R}^{d_y}$ with

$$G_i(x) = \frac{1}{|D_i|} \int_{D_i} u_h(t; x) dt, \quad i = 1, \dots, d_y.$$

Synthetic data for these d_y local averages are produced by $y = G(x_{\text{true}}) + \xi$, where $\xi \sim \mathcal{N}(0, \sigma^2 I_{d_y})$ and x_{true} is a realization of the prior random variable. To investigate the impact of the observation noise in practical applications, we present three test cases with observational standard deviations $\sigma = \{0.034, 0.017, 0.0085\}$ that correspond to signal-to-noise ratios, 10, 20, and 40, respectively. The resulting posterior distribution concentrates with reducing σ .

As shown in Figure 6, for all three test cases, the eigenvalues of the H_k matrices and their gaps decay rapidly, which are similar to the first numerical example. The eigenvalues of H_1 matrices and the associated sums of the residual eigenvalues, $\mathcal{R}(\mathcal{X}_r, H_1)$, are several orders smaller than the eigenvalues of H_0 matrices and $\mathcal{R}(\mathcal{X}_r, H_0)$. In addition, the gap between $\mathcal{R}(\mathcal{X}_r, H_1)$ and $\mathcal{R}(\mathcal{X}_r, H_0)$ increases with decreasing σ . This suggests that the accuracy improvement of the approximate posterior densities induced by the H_1 matrix over those of the H_0 matrix can be further enhanced for more concentrated posterior distributions in this example. Moreover, with a smaller σ , the signal-to-noise ratio is larger, and the posterior density is more different from the prior. As a result, the sampling problem becomes more challenging. This can be observed from the eigenvalue values for $\sigma = 8.5 \times 10^{-3}$, which are several magnitudes larger than the ones of $\sigma = 3.4 \times 10^{-2}$.

In Figure 7, we compare the performance of using H_0 and H_1 with three projection methods and noise scales. The performance is measured in Hellinger distance from the true posterior. We can see that

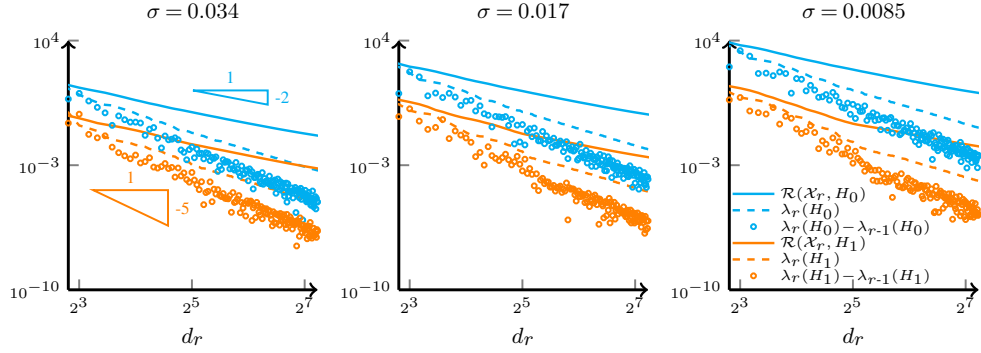


Figure 6. PDE example. Eigenvalues and their gaps of H_k matrices for three test cases with $\sigma = \{0.034, 0.017, 0.0085\}$ and the sums of the residual eigenvalues versus projector dimensions.

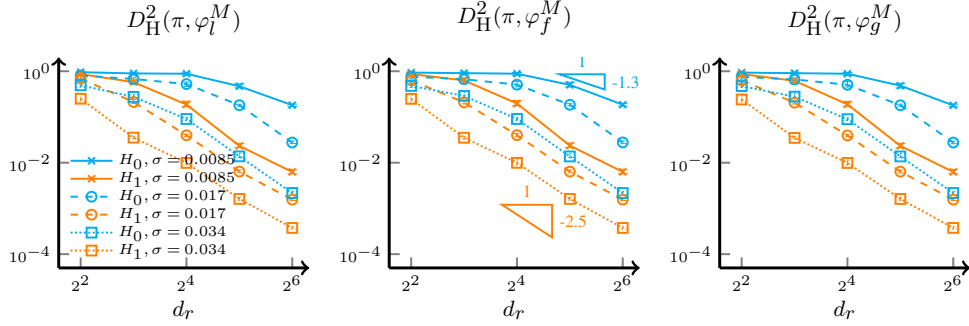


Figure 7. PDE example. Approximation errors of the approximate posterior densities versus projection dimensions for different H_k matrices and different approximation methods. From left to right, approximation methods are φ_l^M , φ_f^M , and φ_g^M , respectively. Sample size $M = 4$ is used in computing the conditional expectation.

all three projection methods yield similar results. Approximations using H_1 consistently outperform the ones using H_0 , especially when d_r increases. By reducing σ , the sampling problem becomes harder, so the approximation becomes less accurate. But this is more severe for the approximations with H_0 , since the approximation error is of order 1 when $d_r = 2^6$ while the approximation error using H_1 is of 10^{-2} when $d_r = 2^6$.

Using the test case with $\sigma = 0.017$, we investigate the impact of sample size m for estimating the lower-dimensional subspace $\hat{\mathcal{X}}_r$. Figure 8 presents the quantiles of the sums of the residual errors for various sample-based subspace estimations. Similar to the first numerical example, the diminishing eigenvalue gaps of H_k matrices (c.f. Figure 6) do not impact the accuracy of subspace estimations. With a rather small sample size $m = 100$, all methods (MC for H_0 and MCMC and SMC for H_1) can lead to accurate subspace estimations.

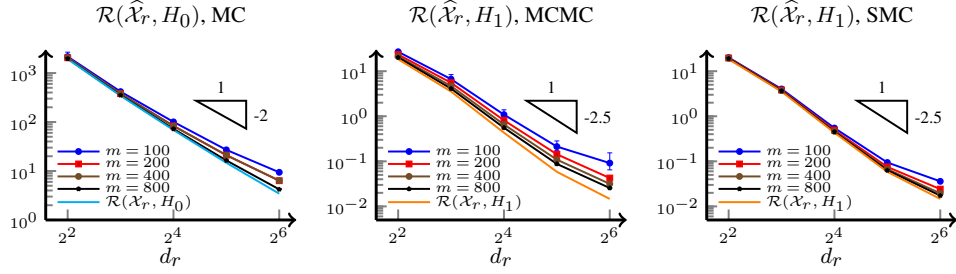


Figure 8. PDE example with $\sigma = 0.017$. The sums of the residual eigenvalues versus projection dimensions for different H_k matrices and subspaces $\hat{\mathcal{X}}_r$ computed using different samples sizes m and different methods. From left to right, we have Monte Carlo estimation of \hat{H}_0 , MCMC estimation of \hat{H}_1 , and SMC estimation of \hat{H}_1 , respectively. The error bars represent [10%, 90%] quantiles estimated using 100 runs.

8. Conclusion

This paper has provided a step-by-step analysis of the accuracy of the LIS method for approximating high-dimensional intractable target probability densities. We have shown that information about the spectrum of the Gram matrices $H_k, k \in \{0, 1\}$, leads to upper bounds on the errors of various true approximations. We have also generalized these upper bounds to the numerical implementation of the approximate probability densities, in which Monte Carlo averaging is applied to both the estimation of $H_k, k \in \{0, 1\}$, and the marginalization used during the construction of the approximate likelihood functions. Our analysis provides insights into the trade-off between the usage of H_0 and H_1 for constructing LIS: while the approximations based on H_1 can have smaller approximation errors compared with those obtained from H_0 , the matrix H_1 is often more difficult to estimate. Fortunately, this difficulty can be addressed by integrating the LIS estimation process into sampling tools such as MCMC and SMC. We have also discussed the performance of the integration of MCMC and SMC with LIS. We have demonstrated our analysis on a linear Bayesian inverse problem, where all the error bounds presented in this paper are independent of the ambient parameter dimension, under suitable technical assumptions that are commonly used in high- or infinite-dimensional inverse problems. Finally, we have provided numerical examples to further demonstrate the efficacy of our analysis on nonlinear problems.

This work leads to some future research directions for dimension reduction techniques. Firstly, our analysis of the linear Bayesian inverse problem shows that various approximation errors are dimension independent. We conjecture this property will also hold for general nonlinear Bayesian inverse problems. Finding the conditions that guarantee this property remains an open problem. Secondly, our analysis indicates that the expected conditional variance of the square root of the likelihood controls the approximation error. This may lead to new dimension reduction techniques that bypass the usage of the Poincaré inequality and the gradient. Moreover, the analysis presented in this work can be further generalized to other types of log-concave reference distributions, for example, the Laplace distribution that is commonly used in sparsity-promoting learning. This may require further investigations on using weighted Poincaré-type inequalities [11, 13] for building alternative H_k matrices and subspace approximations.

Appendix A: Useful lemmas

We begin with several useful lemmas for our discussion. Although some of them are not new, we provide proofs for all lemmas for the sake of completeness.

Lemma A.1. *The following holds*

1) *The estimation error of a L^2 function h can be bounded by Hellinger distance*

$$|\mathbb{E}_\pi[h] - \mathbb{E}_\nu[h]| \leq \sqrt{2\mathbb{E}_\pi[h^2] + 2\mathbb{E}_\nu[h^2]} D_H(\pi, \nu).$$

This result can also be found in [58, Proposition 5.12].

2) *The Hellinger distance can be bounded by the square root of KL divergence*

$$D_H(\pi, \nu) \leq \sqrt{\frac{1}{2} D_{KL}(\pi, \nu)}.$$

This is often referred as the Csiszár-Kullback-Pinsker inequality [14, 63].

3) *The total variation distance can be bounded by the Hellinger distance*

$$D_{TV}(\pi, \nu) \leq \sqrt{2} D_H(\pi, \nu).$$

This is often referred as the Kraft's inequality [55].

Proof. Proof of claim 1). Let λ be a reference density, e.g. the Lebesgue density, for the Hellinger distance, so

$$D_H(\pi, \nu)^2 = \frac{1}{2} \int \left(\sqrt{\frac{\pi(x)}{\lambda(x)}} - \sqrt{\frac{\nu(x)}{\lambda(x)}} \right)^2 \lambda(x) dx.$$

Note that

$$\begin{aligned} |\mathbb{E}_\pi[h] - \mathbb{E}_\nu[h]|^2 &= \left(\int \left(\frac{\pi(x)}{\lambda(x)} - \frac{\nu(x)}{\lambda(x)} \right) h(x) \lambda(x) dx \right)^2 \\ &= \left(\int \left(\sqrt{\frac{\pi(x)}{\lambda(x)}} - \sqrt{\frac{\nu(x)}{\lambda(x)}} \right) \left(\sqrt{\frac{\pi(x)}{\lambda(x)}} + \sqrt{\frac{\nu(x)}{\lambda(x)}} \right) h(x) \lambda(x) dx \right)^2 \\ (\text{by Cauchy-Schwarz}) &\leq D_H(\pi, \nu)^2 \left(\int \left(\sqrt{\frac{\pi(x)}{\lambda(x)}} + \sqrt{\frac{\nu(x)}{\lambda(x)}} \right)^2 h^2(x) \lambda(x) dx \right) \\ (\text{by Young's ineq.}) &\leq D_H(\pi, \nu)^2 \left(\int 2 \left(\frac{\pi(x)}{\lambda(x)} + \frac{\nu(x)}{\lambda(x)} \right) h^2(x) \lambda(x) dx \right) \\ &= 2(\mathbb{E}_\pi[h^2] + \mathbb{E}_\nu[h^2]) D_H(\pi, \nu)^2. \end{aligned}$$

Proof of claim 2). The result comes from the following

$$D_{KL}(\pi, \nu) = \int \log \frac{\pi(x)}{\nu(x)} \pi(x) dx$$

$$\begin{aligned}
&= -2 \int \log \frac{\sqrt{\nu(x)}}{\sqrt{\pi(x)}} \pi(x) dx \\
(\text{by } -\log(1+x) \geq -x) &\geq -2 \int \left(\frac{\sqrt{\nu(x)}}{\sqrt{\pi(x)}} - 1 \right) \pi(x) dx \\
&= \int (\pi(x) + \pi(x) - 2\sqrt{\pi(x)\nu(x)}) dx \\
&= \int (\pi(x) + \nu(x) - 2\sqrt{\pi(x)\nu(x)}) dx = 2D_H(\pi, \nu)^2.
\end{aligned}$$

Proof of claim 3). The result comes from the following

$$\begin{aligned}
D_{TV}(\pi, \nu)^2 &= \left(\frac{1}{2} \int \left| \frac{\pi(x)}{\lambda(x)} - \frac{\nu(x)}{\lambda(x)} \right| \lambda(x) dx \right)^2 \\
&\leq \left(\frac{1}{2} \int \left(\sqrt{\frac{\pi(x)}{\lambda(x)}} - \sqrt{\frac{\nu(x)}{\lambda(x)}} \right)^2 \lambda(x) dx \right) \left(\frac{1}{2} \int \left(\sqrt{\frac{\pi(x)}{\lambda(x)}} + \sqrt{\frac{\nu(x)}{\lambda(x)}} \right)^2 \lambda(x) dx \right) \\
&\leq D_H(\pi, \nu)^2 \int \left(\frac{\pi(x)}{\lambda(x)} + \frac{\nu(x)}{\lambda(x)} \right) \lambda(x) dx = 2D_H(\pi, \nu)^2.
\end{aligned}$$

□

Lemma A.2. Consider two probability densities $\pi(x) = \frac{1}{Z_f} f(x) \mu(x)$ and $p(x) = \frac{1}{Z_h} h(x) \mu(x)$ where $Z_f = \int f(x) \mu(x) dx$ and $Z_h = \int h(x) \mu(x) dx$. Given the L^2 distance between \sqrt{f} and \sqrt{h}

$$\|\sqrt{f} - \sqrt{h}\|_{2,\mu} = \left(\int (\sqrt{f(x)} - \sqrt{h(x)})^2 \mu(x) dx \right)^{\frac{1}{2}}.$$

Then we have the following:

- 1) The normalizing constant difference is bounded as $|\sqrt{Z_f} - \sqrt{Z_h}| \leq \|\sqrt{f} - \sqrt{h}\|_{2,\mu}$.
- 2) The squared Hellinger distance is bounded as $D_H(\pi, p)^2 \leq \frac{2}{Z_f} \|\sqrt{f} - \sqrt{h}\|_{2,\mu}^2$.

Proof. Proof of claim 1). Note that

$$\begin{aligned}
|Z_f - Z_h| &= \left| \int (f(x) - h(x)) \mu(x) dx \right| \\
&= \left| \int (\sqrt{f(x)} - \sqrt{h(x)}) (\sqrt{f(x)} + \sqrt{h(x)}) \mu(x) dx \right| \\
&\leq \left| \int (\sqrt{f(x)} - \sqrt{h(x)})^2 \mu(x) dx \right|^{1/2} \left| \int (\sqrt{f(x)} + \sqrt{h(x)})^2 \mu(x) dx \right|^{1/2} \\
&\leq \left| \int (\sqrt{f(x)} - \sqrt{h(x)})^2 \mu(x) dx \right|^{1/2} \left(\left| \int f(x) \mu(x) dx \right|^{1/2} + \left| \int h(x) \mu(x) dx \right|^{1/2} \right)
\end{aligned}$$

$$= (\sqrt{Z_f} + \sqrt{Z_h}) \left| \int (\sqrt{f(x)} - \sqrt{h(x)})^2 \mu(x) dx \right|^{1/2}$$

Dividing both sides by $(\sqrt{Z_f} + \sqrt{Z_h}) > 0$ we have the result.

Proof of claim 2). The squared Hellinger distance of π from p satisfies

$$\begin{aligned} D_H^2(\pi, p) &= \frac{1}{2} \int (\sqrt{\pi(x)} - \sqrt{p(x)})^2 dx \\ &= \frac{1}{2} \int \left(\sqrt{\frac{f(x)}{Z_f}} - \sqrt{\frac{h(x)}{Z_h}} \right)^2 \mu(x) dx \\ &= \frac{1}{2Z_f} \int \left(\sqrt{f(x)} - \sqrt{h(x)} + \sqrt{h(x)} - \sqrt{h(x)} \sqrt{\frac{Z_f}{Z_h}} \right)^2 \mu(x) dx \\ &= \frac{1}{2Z_f} \int \left(\sqrt{f(x)} - \sqrt{h(x)} + \sqrt{h(x)} \left(1 - \sqrt{\frac{Z_f}{Z_h}} \right) \right)^2 \mu(x) dx \\ (\text{by Young's ineq.}) &\leq \frac{1}{Z_f} \left(\int (\sqrt{f(x)} - \sqrt{h(x)})^2 \mu(x) dx + \left| 1 - \sqrt{\frac{Z_f}{Z_h}} \right|^2 \int h(x) \mu(x) dx \right) \\ &= \frac{1}{Z_f} \left(\|\sqrt{f} - \sqrt{h}\|_{\mu}^2 + \left| \sqrt{Z_h} - \sqrt{Z_f} \right|^2 \right) \leq \frac{2}{Z_f} \|\sqrt{f} - \sqrt{h}\|_{2, \mu}^2. \end{aligned}$$

Thus, the result follows. \square

Lemma A.3. Let $C \in \mathbb{R}^{d \times d}$ be symmetric and positive semidefinite, $U \in \mathbb{R}^{d \times d}$ be a rank p symmetric matrix, for $p \geq 1$. Then for any k

$$\lambda_{k+p}(C + U) \leq \lambda_k(C).$$

Proof. By the Courant–Fischer–Weyl min-max principle, we note that for any symmetric matrix C

$$\lambda_{k+p}(C + U) = \min_V \{ \max \{ x^\top (C + U)x, \|x\| = 1, x \in V \}, \dim(V) = d - k - p + 1 \}.$$

Let the eigenvectors of C be v_1, \dots, v_d and the eigenvectors of U with nonzero eigenvalues be u_1, \dots, u_p . Now we pick

$$V_\perp = \text{span}\{v_1, \dots, v_{k-1}, u_1, \dots, u_p\},$$

and its orthogonal complement V' as a subspace of dimension at least $d - k - p + 1$. Select any subspace V of dimension $d - k - p + 1$ from V' , then

$$\lambda_{k+p}(C + U) \leq \max_{x \in V, \|x\|=1} x^\top (C + U)x = \max_{x \in V, \|x\|=1} x^\top Cx \leq \lambda_k(C).$$

\square

Appendix B: Proofs in Section 2

B.1. Proof of Proposition 2.2

Denote the density $\nu(x) \propto \exp(-V(x))$ and the associated conditional density as $\nu(x_\perp|x_r)$. Note that

$$\mu(x_\perp|x_r) = \frac{\mu(x_r, x_\perp)}{\int \mu(x_r, x_\perp) dx_\perp} = \frac{\exp(-V(x_r, x_\perp)) \exp(-U(x_r, x_\perp))}{\int \exp(-V(x_r, x_\perp)) \exp(-U(x_r, x_\perp)) dx_\perp}.$$

Let $c_0 = \inf_x \exp(-U(x))$. Then $\exp(-U(x_r, x_\perp)) \leq Bc_0$, so

$$\mu(x_\perp|x_r) \leq \frac{\exp(-V(x_r, x_\perp)) Bc_0}{\int \exp(-V(x_r, x_\perp)) c_0 dx_\perp} = B\nu(x_\perp|x_r).$$

Likewise

$$\mu(x_\perp|x_r) \geq \frac{\exp(-V(x_r, x_\perp)) c_0}{\int \exp(-V(x_r, x_\perp)) c_0 B dx_\perp} = B^{-1}\nu(x_\perp|x_r).$$

Finally, note that

$$-\nabla_{x_\perp}^2 \log \nu(x_\perp|x_r) = -\nabla_{x_\perp}^2 \log \nu(x_\perp, x_r),$$

which is a sub-matrix of $-\nabla^2 \log \nu(x)$, so its minimal eigenvalue is greater than c by the assumption of strong log-concavity. Then the Bakry–Emery principle (see, e.g. Theorem 3.1 of [44]) indicates that $\nu(x_\perp|x_r)$ satisfies the Poincaré inequality with coefficient c , i.e. for any $h \in C^1$

$$\text{var}_{\nu(x_\perp|x_r)}[h] \leq \frac{1}{c} \int \|\nabla h(x_r, x_\perp)\|^2 \nu(x_\perp|x_r) dx_\perp.$$

Finally, we have the Poincaré inequality for $\mu(x_\perp|x_r)$:

$$\begin{aligned} \text{var}_{\mu(x_\perp|x_r)}[h] &\leq \int [h(x) - \mathbb{E}_{\nu(x_\perp|x_r)}[h(x)]]^2 \mu(x_\perp|x_r) dx_\perp \\ &\leq B \int [h(x) - \mathbb{E}_{\nu(x_\perp|x_r)}[h(x)]]^2 \nu(x_\perp|x_r) dx_\perp \\ &= B \text{var}_{\nu(x_\perp|x_r)}(h) \\ &\leq \frac{B}{c} \int \|\nabla_{x_\perp} h(x_r, x_\perp)\|^2 \nu(x_\perp|x_r) dx_\perp \\ &\leq \frac{B^2}{c} \int \|\nabla_{x_\perp} h(x_r, x_\perp)\|^2 \mu(x_\perp|x_r) dx_\perp. \end{aligned}$$

□

B.2. Proof of Proposition 2.3

Proof of claim 1). Recall the squared Hellinger distance

$$D_H(\pi, \varphi_f)^2 = \frac{1}{2} \int \left(\sqrt{\frac{\pi(x)}{\mu(x)}} - \sqrt{\frac{\varphi_f(x)}{\mu(x)}} \right)^2 \mu(x) dx$$

$$= \frac{1}{Z} \int \left(\frac{1}{2} \int (f(x_r, x_\perp)^{\frac{1}{2}} - \bar{f}(x_r)^{\frac{1}{2}})^2 \mu(x_\perp | x_r) dx_\perp \right) \bar{\mu}(x_r) dx_r, \quad (18)$$

and definitions of $\bar{f}(x_r)$ and $\bar{g}(x_r)$:

$$\bar{f}(x_r) = \int g(x_r, x_\perp)^2 \mu(x_\perp | x_r) dx_\perp, \quad \bar{g}(x_r) = \int g(x_r, x_\perp) \mu(x_\perp | x_r) dx_\perp.$$

We have the identity:

$$\text{var}_{\mu(x_\perp | x_r)}[g] = \bar{f}(x_r) - \bar{g}(x_r)^2. \quad (19)$$

The inner integral in (18) can be expressed as

$$\begin{aligned} & \frac{1}{2} \int (g(x_r, x_\perp) - \bar{f}(x_r)^{\frac{1}{2}})^2 \mu(x_\perp | x_r) dx_\perp \\ &= \frac{1}{2} \int (g(x_r, x_\perp)^2 + \bar{f}(x_r) - 2g(x_r, x_\perp) \bar{f}(x_r)^{\frac{1}{2}}) \mu(x_\perp | x_r) dx_\perp \\ &= \bar{f}(x_r) - \bar{f}(x_r)^{\frac{1}{2}} \bar{g}(x_r). \end{aligned}$$

By the Cauchy–Schwarz inequality, we have $\bar{f}(x_r)^{\frac{1}{2}} \geq \bar{g}(x_r) \geq 0$, and therefore

$$\bar{f}(x_r) \geq \bar{f}(x_r)^{\frac{1}{2}} \bar{g}(x_r) \geq \bar{g}(x_r)^2 \geq 0.$$

This leads to the inequality

$$\bar{f}(x_r) - \bar{f}(x_r)^{\frac{1}{2}} \bar{g}(x_r) \leq \bar{f}(x_r) - \bar{g}(x_r)^2 = \text{var}_{\mu(x_\perp | x_r)}[g].$$

Applying this bound above to (18), we find that:

$$D_H(\pi, \varphi_f)^2 \leq \frac{1}{Z} \int \text{var}_{\mu(x_\perp | x_r)}[g] \bar{\mu}(x_r) dx_r.$$

Proof of claim 2). Recall that the normalizing constant of φ_g takes the form

$$Z_g := \int \bar{g}(x_r)^2 \mu(x) dx.$$

The squared Hellinger distance can be written as

$$D_H(\pi, \varphi_g)^2 = \frac{1}{2} \int \left(\int \left(\frac{1}{Z^{\frac{1}{2}}} g(x_r, x_\perp) - \frac{1}{Z_g^{\frac{1}{2}}} \bar{g}(x_r) \right)^2 \mu(x_\perp | x_r) dx_\perp \right) \bar{\mu}(x_r) dx_r. \quad (20)$$

Using the identity (19) and $\bar{f}(x_r)^{\frac{1}{2}} \geq \bar{g}(x_r) \geq 0$, we have

$$Z = \int f(x) \mu(x) dx = \int \bar{f}(x_r) \bar{\mu}(x_r) dx_r \geq \int \bar{g}(x_r)^2 \bar{\mu}(x_r) dx_r = \int \bar{g}(x_r)^2 \mu(x) dx = Z_g > 0,$$

and therefore $\frac{Z_g}{Z} \leq 1$. Then, we can bound the inner integral in (20) by

$$\begin{aligned}
\int \left(\frac{1}{Z^{\frac{1}{2}}} g(x_r, x_\perp) - \frac{1}{Z_g^{\frac{1}{2}}} \bar{g}(x_r) \right)^2 \mu(x_\perp | x_r) dx_\perp &= \frac{1}{Z} \left(\bar{f}(x_r) + \frac{Z}{Z_g} \bar{g}(x_r)^2 - 2\sqrt{\frac{Z}{Z_g}} \bar{g}(x_r)^2 \right) \\
&\leq \frac{1}{Z} \left(\bar{f}(x_r) + \frac{Z}{Z_g} \bar{g}(x_r)^2 - 2\bar{g}(x_r)^2 \right) \\
&= \frac{1}{Z} \left(\bar{f}(x_r) + \frac{Z - Z_g}{Z_g} \bar{g}(x_r)^2 - \bar{g}(x_r)^2 \right) \\
&= \frac{1}{Z} \left(\text{var}_{\mu(x_\perp | x_r)}[g] + \frac{Z - Z_g}{Z_g} \bar{g}(x_r)^2 \right).
\end{aligned}$$

Substituting this upper bound into (20), we have

$$\begin{aligned}
D_H(\pi, \varphi_g)^2 &\leq \frac{1}{2Z} \int \left(\text{var}_{\mu(x_\perp | x_r)}[g] + \frac{Z - Z_g}{Z_g} \bar{g}(x_r)^2 \right) \bar{\mu}(x_r) dx_r \\
&= \frac{1}{2Z} \left(\int \text{var}_{\mu(x_\perp | x_r)}[g] \bar{\mu}(x_r) dx_r + (Z - Z_g) \right).
\end{aligned}$$

The term $Z - Z_g$ satisfies

$$\begin{aligned}
Z - Z_g &= \int \left(\int (g(x_r, x_\perp)^2 - \bar{g}(x_r)^2) \mu(x_\perp | x_r) dx_\perp \right) \bar{\mu}(x_r) dx_r \\
&= \int \text{var}_{\mu(x_\perp | x_r)}[g] \bar{\mu}(x_r) dx_r.
\end{aligned} \tag{21}$$

In summary, we have

$$D_H(\pi, \varphi_g)^2 \leq \frac{1}{Z} \left(\int \text{var}_{\mu(x_\perp | x_r)}[g] \bar{\mu}(x_r) dx_r \right).$$

□

B.3. Proof of Theorem 2.4

Claim 1). Recall that in (2), the projector P_r satisfies $\text{range}(P_r) = \mathcal{X}_r$. By the Poincaré inequality of $\mu(x_\perp | x_r)$, the expected conditional variance of g satisfies

$$\text{var}_{\mu(x_\perp | x_r)}[g] \leq \kappa \int \|(I - P_r)\nabla g(x)\|^2 \mu(x_\perp | x_r) dx_\perp.$$

Applying Proposition 2.3, we have

$$\begin{aligned}
D_H(\pi, \varphi_f)^2 &\leq \frac{\kappa}{Z} \int \left(\int \|(I - P_r)\nabla g(x)\|^2 \mu(x_\perp | x_r) dx_\perp \right) \mu(x_r) dx_r \\
&= \frac{\kappa}{Z} \int \|(I - P_r)\nabla g(x)\|^2 \mu(x) dx
\end{aligned}$$

$$\begin{aligned}
&= \frac{\kappa}{Z} \int \|P_{\perp} \nabla \log g(x)\|^2 g(x)^2 \mu(x) dx \\
&= \frac{\kappa}{4} \int \|P_{\perp} \nabla \log f(x)\|^2 \pi(x) dx.
\end{aligned}$$

Since $\|P_{\perp} \nabla \log f(x)\|^2 = P_{\perp} \nabla \log f(x) \nabla \log f(x)^{\top} P_{\perp}$, the result follows from

$$\int \|P_{\perp} \nabla \log f(x)\|^2 \pi(x) dx = \mathcal{R}(\mathcal{X}_r, H_1).$$

Claim 2). This result follows from Lemma A.1 and claim 1).

Claim 3). The same proofs of claims 1) and 2) can be applied. \square

B.4. Proof of Theorem 2.6

Proof of claim 1). Note that

$$\begin{aligned}
\int (\log f(x) - \bar{l}(x_r))^2 \mu(x_{\perp} | x_r) dx_{\perp} &= \text{var}_{\mu(x_{\perp} | x_r)}[\log f(x)] \\
&\leq \kappa \int \|\nabla_{x_{\perp}} \log f(x_{\perp}, x_r)\|^2 \mu(x_{\perp} | x_r) dx_{\perp} \\
&= \kappa \int \|P_{\perp} \nabla \log f(x)\|^2 \mu(x_{\perp} | x_r) dx_{\perp}.
\end{aligned}$$

Integrating both sides with respect to $\bar{\mu}(x_r)$ yields

$$\int (\log f(x) - \bar{l}(x_r))^2 \mu(x) dx \leq \kappa \mathcal{R}(\mathcal{X}_r, H_0).$$

Then by the Cauchy–Schwarz inequality, we find

$$\int (\log f(x) - \bar{l}(x_r))^2 \mu(x) dx \int f^2(x) \mu(x) dx \geq Z^2 \left(\int \log \frac{\pi(x)Z}{\varphi_l(x)Z_l} \pi(x) dx \right)^2,$$

where

$$\begin{aligned}
Z_l &:= \int \exp(\bar{l}(x_r)) \bar{\mu}(x_r) dx_r \\
&= \int \exp\left(\int \log f(x) \mu(x_{\perp} | x_r) dx_{\perp}\right) \bar{\mu}(x_r) dx_r \\
&\leq \int \left(\int f(x) \mu(x_{\perp} | x_r) dx_{\perp}\right) \bar{\mu}(x_r) dx_r = Z. \quad (\text{by Jensen's ineq.})
\end{aligned}$$

Moreover, it is well known that $D_{KL}(\pi, \varphi_l) = \int \log \frac{\pi(x)}{\varphi_l(x)} \pi(x) dx \geq 0$, so

$$\left(\int \log \frac{\pi(x)Z}{\varphi_l(x)Z_l} \pi(x) dx \right)^2 = (D_{KL}(\pi, \varphi_l) + \log Z/Z_l)^2 \geq D_{KL}^2(\pi, \varphi_l).$$

In conclusion, we have claim 1) by

$$\begin{aligned} D_{KL}^2(\pi, \varphi_l) &\leq \left(\int \log \frac{\pi(x)Z}{\varphi_l(x)Z_l} \pi(x) dx \right)^2 \\ &\leq \frac{1}{Z^2} \int (\log f(x) - \bar{l}(x_r))^2 \mu(x) dx \int f^2(x) \mu(x) dx \\ &\leq \frac{\|f\|_{2,\mu}^2 \kappa}{Z^2} \int \|P_\perp \nabla \log f(x)\|^2 \mu(x) dx = \frac{\|f\|_{2,\mu}^2 \kappa}{Z^2} \mathcal{R}(\mathcal{X}_r, H_0). \end{aligned}$$

Proof of claim 2). Applying claim 1) of Lemma A.1, claim 2) of Lemma A.1, and then claim 1) of Theorem 2.6, we have

$$\begin{aligned} |\mathbb{E}_\pi[h] - \mathbb{E}_{\varphi_l}[h]| &\leq \sqrt{2(\mathbb{E}_\pi[h^2] + \mathbb{E}_{\varphi_l}[h^2])} D_H(\pi, \varphi_l) \\ &\leq (\mathbb{E}_\pi[h^2] + \mathbb{E}_{\varphi_l}[h^2])^{\frac{1}{2}} \sqrt{D_{KL}(\pi, \varphi_l)} \\ &\leq (\mathbb{E}_\pi[h^2] + \mathbb{E}_{\varphi_l}[h^2])^{\frac{1}{2}} \sqrt{\frac{\|f\|_{2,\mu}^2 \kappa}{Z} (\mathcal{R}(\mathcal{X}_r, H_0))^{\frac{1}{4}}}. \end{aligned}$$

Thus, the result follows. \square

Appendix C: Proofs in Section 3

C.1. Proof of Theorem 3.1

Proof of claim 1). Recalling the function g takes the form $g = \sqrt{f}$ and using

$$\bar{g}^M(x_r) = \frac{1}{M} \sum_{i=1}^M g(x_r, X_\perp^i) = \frac{1}{M} \sum_{i=1}^M g(x_r, T(x_r, W^i)), \quad \text{and} \quad \bar{g}(x_r) = \int g(x_r, x_\perp) \mu(x_\perp | x_r) dx_\perp,$$

we have the corresponding approximate target densities $\varphi_g^M(x_r, x_\perp) \propto \bar{g}^M(x_r)^2 \mu(x_r, x_\perp)$ and $\varphi_g(x_r, x_\perp) \propto \bar{g}(x_r)^2 \mu(x_r, x_\perp)$, respectively. Note that

$$\mathbb{E}_M[\bar{g}^M(x_r)] = \frac{1}{M} \sum_{i=1}^M \mathbb{E}_M g(x_r, T(x_r, W^i)) = \bar{g}(x_r),$$

$$\mathbb{E}_M[(\bar{g}^M(x_r) - \bar{g}(x_r))^2] = \frac{1}{M} \sum_{i=1}^M \text{var}_M[g(x_r, T(x_r, W^i))] = \text{var}_{\mu(x_\perp | x_r)}[g(x_r, x_\perp)].$$

Applying Lemma A.2 claim 2), we have

$$\begin{aligned} \mathbb{E}_M [D_H(\varphi_g^M, \varphi_g)^2] &\leq \frac{2}{Z_g} \mathbb{E}_M \left[\int \int (\bar{g}^M(x_r) - \bar{g}(x_r))^2 \bar{\mu}(x_r) dx_r \mu(x_\perp | x_r) dx_\perp \right] \\ &= \frac{2}{Z_g M} \int \text{var}_{\mu(x_\perp | x_r)}(g(x_r, x_\perp)) \bar{\mu}(x_r) dx_r \end{aligned}$$

$$\begin{aligned}
&\leq \frac{2\kappa}{Z_g M} \int \|\nabla_{x_\perp} g(x)\|^2 \mu(x) dx \\
&= \frac{2\kappa}{Z_g M} \int \|\nabla_{x_\perp} \log g(x)\|^2 f(x) \mu(x) dx \\
&= \frac{2\kappa Z}{Z_g M} \mathcal{R}(\mathcal{X}_r, H_1).
\end{aligned}$$

Thus, the result follows from Jensen's inequality.

Proof of claim 2). We have the corresponding approximate target densities $\varphi_f^M(x_r, x_\perp) \propto \bar{f}^M(x_r) \mu(x_r, x_\perp)$ and $\varphi_f(x_r, x_\perp) = \frac{1}{Z} \bar{f}(x_r) \mu(x_r, x_\perp)$ where

$$\bar{f}^M(x_r) = \frac{1}{M} \sum_{i=1}^M f(x_r, X_\perp^i) = \frac{1}{M} \sum_{i=1}^M f(x_r, T(x_r, W^i)), \quad \text{and} \quad \bar{f}(x_r) = \int f(x_r, x_\perp) \mu(x_\perp | x_r) dx_\perp.$$

Similar to the proof of claim 1), we apply Lemma A.2 claim 2) and find

$$\begin{aligned}
\mathbb{E}_M \left[D_H(\varphi_f^M, \varphi_f)^2 \right] &\leq \frac{2}{Z} \mathbb{E}_M \left[\int \int (\sqrt{\bar{f}^M(x_r)} - \sqrt{\bar{f}(x_r)})^2 \mu(x_r, x_\perp) dx_r dx_\perp \right] \\
&= \frac{2}{Z} \mathbb{E}_M \left[\int \int (\sqrt{\bar{f}^M(x_r)} - \sqrt{\bar{f}(x_r)})^2 \bar{\mu}(x_r) dx_r \mu(x_\perp | x_r) dx_\perp \right] \\
&= \frac{2}{Z} \int \mathbb{E}_M \left[(\sqrt{\bar{f}^M(x_r)} - \sqrt{\bar{f}(x_r)})^2 \right] \bar{\mu}(x_r) dx_r, \tag{22}
\end{aligned}$$

here. Considering the identity

$$\begin{aligned}
(\sqrt{\bar{f}^M(x_r)} - \sqrt{\bar{f}(x_r)})^2 &\leq (\sqrt{\bar{f}^M(x_r)} - \sqrt{\bar{f}(x_r)})^2 (\sqrt{\bar{f}^M(x_r)/\bar{f}(x_r)} + 1)^2 \\
&= (\bar{f}^M(x_r) - \bar{f}(x_r))^2 / \bar{f}(x_r),
\end{aligned}$$

the inequality in (22) also satisfies

$$\mathbb{E}_M \left[D_H(\varphi_f^M, \varphi_f)^2 \right] \leq \frac{2}{Z} \int \frac{\mathbb{E}_M [(\bar{f}^M(x_r) - \bar{f}(x_r))^2]}{\bar{f}(x_r)} \bar{\mu}(x_r) dx_r. \tag{23}$$

Then for each given x_r , by independence of x_\perp^i we have

$$\begin{aligned}
\mathbb{E}_M \left[(\bar{f}^M(x_r) - \bar{f}(x_r))^2 \right] &= \frac{1}{M} \text{var}_{\mu(x_\perp | x_r)} f(x_r, x_\perp) \\
&\leq \frac{\kappa}{M} \int \|\nabla_{x_\perp} f(x_r, x_\perp)\|^2 \mu(x_\perp | x_r) dx_\perp \\
&= \frac{\kappa}{M} \int \|\nabla_{x_\perp} \log f(x_r, x_\perp)\|^2 f(x_r, x_\perp) \mu(x_\perp | x_r) dx_\perp \\
&= \frac{\kappa}{M} \bar{f}(x_r)^2 \int \|\nabla_{x_\perp} \log f(x_r, x_\perp)\|^2 f(x_\perp | x_r) \mu(x_\perp | x_r) dx_\perp.
\end{aligned}$$

Substituting the above identify into (23), we have

$$\begin{aligned}\mathbb{E}_M \left[D_H(\varphi_f^M, \varphi_f)^2 \right] &\leq \frac{2\kappa}{ZM} \int \int \|\nabla_{x_\perp} \log f(x)\|^2 f(x_\perp|x_r)^2 \mu(x_\perp|x_r) dx_\perp \bar{f}(x_r) \bar{\mu}(x_r) dx_r \\ &= \frac{2\kappa}{ZM} \int \|\nabla_{x_\perp} \log f(x)\|^2 f(x_\perp|x_r) f(x) \mu(x) dx \\ &\leq \frac{2\kappa C_f}{M} \mathcal{R}(\mathcal{X}_r, H_1),\end{aligned}$$

where $C_f = \sup_{x_r} \sup_{x_\perp} f(x_\perp|x_r)$. Then, the result follows from Jensen's inequality. \square

C.2. Proof of Theorem 3.2

By the independence of the Monte Carlo samples, we have

$$\begin{aligned}\mathbb{E}_M \left[(\bar{l}^M(x_r) - \bar{l}(x_r))^2 \right] &= \mathbb{E}_M \left[\left(\frac{1}{M} \sum_{i=1}^M l(x_r, T(x_r, W^i)) - \bar{l}(x_r) \right)^2 \right] \\ &= \frac{1}{M} \text{var}_{\mu(x_\perp|x_r)} [l(x_r, x_\perp)],\end{aligned}$$

which leads to the following using Assumption 2.1,

$$\mathbb{E}_M \left[\int (\bar{l}^M(x_r) - \bar{l}(x_r))^2 \bar{\mu}(x_r) dx_r \right] \leq \frac{\kappa}{M} \int \text{var}_{\mu(x_\perp|x_r)} [l(x_r, x_\perp)] \bar{\mu}(x_r) dx_r.$$

By Jensen's inequality, the expected L^2 error of $\bar{l}^M(x_r)$ satisfies

$$\mathbb{E}_M \left[\left(\int (\bar{l}^M(x_r) - \bar{l}(x_r))^2 \bar{\mu}(x_r) dx_r \right)^{\frac{1}{2}} \right] \leq \frac{\sqrt{\kappa}}{\sqrt{M}} \left(\int \text{var}_{\mu(x_\perp|x_r)} [l(x_r, x_\perp)] \bar{\mu}(x_r) dx_r \right)^{\frac{1}{2}}. \quad (24)$$

Assumption 2.1 states that

$$\int \text{var}_{\mu(x_\perp|x_r)} [l(x_r, x_\perp)] \bar{\mu}(x_r) dx_r \leq \kappa \int \int \|\nabla_{x_\perp} l(x_r, x_\perp)\|^2 \mu(x_\perp|x_r) dx_\perp \bar{\mu}(x_r) dx_r = \kappa \mathcal{R}(\mathcal{X}_r, H_0),$$

together with (24), we have

$$\mathbb{E}_M \left[\left(\int (\bar{l}^M(x_r) - \bar{l}(x_r))^2 \bar{\mu}(x_r) dx_r \right)^{\frac{1}{2}} \right] \leq \frac{\sqrt{\kappa}}{\sqrt{M}} \sqrt{\mathcal{R}(\mathcal{X}_r, H_0)}.$$

To obtain the KL divergence, we note that

$$\begin{aligned}\mathbb{E}_M \left[D_{KL}(\pi, \varphi_l^M) \right] &= \mathbb{E}_M \left[\int \log \frac{\pi(x)}{\varphi_l^M(x)} \pi(x) dx \right] \\ &= \mathbb{E}_M \left[\int (l(x) - \bar{l}^M(x_r)) \pi(x) dx \right] + \mathbb{E}_M \left[\log \frac{ZM}{Z} \right],\end{aligned}$$

where $Z_M = \int e^{\bar{l}^M(x_r)} \bar{\mu}(x_r) dx_r$. The expectation of Z_M satisfies

$$\begin{aligned}
\mathbb{E}_M[Z_M] &= \mathbb{E}_M \left[\int e^{\bar{l}^M(x_r)} \bar{\mu}(x_r) dx_r \right] \\
&= \int \mathbb{E}_M \left[\exp \left(\frac{1}{M} \sum_{i=1}^M l(x_r, x_{\perp}^i) \right) \right] \bar{\mu}(x_r) dx_r \\
&\leq \int \left(\mathbb{E}_M \left[\prod_{i=1}^M \exp \left(l(x_r, x_{\perp}^i) \right) \right] \right)^{1/M} \bar{\mu}(x_r) dx_r \\
&= \int \left(\prod_{i=1}^M \int \exp \left(l(x_r, x_{\perp}^i) \right) \mu(x_{\perp}^i | x_r) dx_{\perp}^i \right)^{1/M} \bar{\mu}(x_r) dx_r \\
&= \int \int f(x_r, x_{\perp}) \mu(x_{\perp} | x_r) dx_{\perp} \bar{\mu}(x_r) dx_r = Z.
\end{aligned}$$

Therefore, by Jensen's inequality, we have

$$\mathbb{E}_M \left[\log \frac{Z_M}{Z} \right] \leq \log \mathbb{E}_M \left[\frac{Z_M}{Z} \right] \leq 0.$$

Thus, the expected KL satisfies

$$\begin{aligned}
\mathbb{E}_M [D_{KL}(\pi, \varphi_l^M)] &\leq \mathbb{E}_M \left[\int \left(l(x) - \bar{l}(x_r) + \bar{l}(x_r) - \bar{l}^M(x_r) \right) \pi(x) dx \right] \\
&= \int \left(l(x) - \bar{l}(x_r) \right) \pi(x) dx + \mathbb{E}_M \left[\int \left(\bar{l}(x_r) - \bar{l}^M(x_r) \right) \pi(x) dx \right]. \quad (25)
\end{aligned}$$

Applying the Cauchy–Schwarz inequality, the first term in (25) can be bounded by

$$\begin{aligned}
\int \left(l(x) - \bar{l}(x_r) \right) \pi(x) dx &\leq \frac{\|f\|_{2,\mu}}{Z} \left(\int \left(l(x) - \bar{l}(x_r) \right)^2 \mu(x) dx \right)^{\frac{1}{2}} \\
&= \frac{\|f\|_{2,\mu}}{Z} \left(\int \text{var}_{\mu(x_{\perp}|x_r)} [l(x_r, x_{\perp})] \bar{\mu}(x_r) dx_r \right)^{\frac{1}{2}},
\end{aligned}$$

and the second term in (25) can be bounded by

$$\mathbb{E}_M \left[\int \left(\bar{l}(x_r) - \bar{l}^M(x_r) \right) \pi(x) dx \right] \leq \frac{\|f\|_{2,\mu}}{Z} \mathbb{E}_M \left[\left(\int \left(\bar{l}(x_r) - \bar{l}^M(x_r) \right)^2 \bar{\mu}(x_r) dx_r \right)^{\frac{1}{2}} \right].$$

Thus, applying the bound on $\mathbb{E}_M[\cdot]$ in (24) and Assumption 2.1, we have

$$\begin{aligned}
\mathbb{E}_M [D_{KL}(\pi, \varphi_l^M)] &\leq \frac{\|f\|_{2,\mu}}{Z} \left(1 + \frac{1}{\sqrt{M}} \right) \left(\int \text{var}_{\mu(x_{\perp}|x_r)} [l(x_r, x_{\perp})] \bar{\mu}(x_r) dx_r \right)^{1/2} \\
&\leq \frac{\|f\|_{2,\mu}}{Z} \left(1 + \frac{1}{\sqrt{M}} \right) \left(\kappa \int \|\nabla_{x_{\perp}} l(x_r, x_{\perp})\|^2 \mu(x) dx \right)^{1/2}
\end{aligned}$$

$$= \frac{\sqrt{\kappa} \|f\|_{2,\mu}}{Z} \left(1 + \frac{1}{\sqrt{M}}\right) \sqrt{\mathcal{R}(\mathcal{X}_r, H_0)}.$$

□

Appendix D: Proofs in Section 4

D.1. Proof of Lemma 4.1

Given two positive semidefinite matrices $\Sigma, \widehat{\Sigma} \in \mathbb{R}^{d \times d}$, let \widehat{V}_r be the matrix consisting of the d_r leading orthonormal eigenvectors of $\widehat{\Sigma}$ such that $\widehat{V}_r^\top \widehat{V}_r = I_{d_r}$, and $\widehat{\Lambda}_r$ be the $d_r \times d_r$ diagonal matrices consisting of the d_r leading eigenvalues of $\widehat{\Sigma}$ as its diagonal entries. Similarly, let V_r and Λ_r be the matrices consisting of the d_r leading orthonormal eigenvectors of Σ and the d_r leading eigenvalues of Σ , respectively. We can define the orthogonal projectors $\widehat{P}_r = \widehat{V}_r \widehat{V}_r^\top$ and $\widehat{P}_\perp = I - \widehat{P}_r$.

Proof of claim 1). Since $\text{tr}(\widehat{P}_\perp \Sigma \widehat{P}_\perp) = \text{tr}(\Sigma \widehat{P}_\perp^2) = \text{tr}(\Sigma \widehat{P}_\perp) = \text{tr}(\Sigma) - \text{tr}(\Sigma \widehat{P}_r)$, we have

$$\begin{aligned} \text{tr}(\widehat{P}_\perp \Sigma \widehat{P}_\perp) &= \text{tr}(\Sigma) - \text{tr}(\Lambda_r) + \text{tr}(\Lambda_r) - \text{tr}(\Sigma \widehat{P}_r) + \text{tr}(\widehat{\Sigma} \widehat{P}_r) - \text{tr}(\widehat{\Sigma} \widehat{P}_r) \\ &= \text{tr}(\Sigma) - \text{tr}(\Lambda_r) + \text{tr}(\Lambda_r) - \text{tr}(\widehat{\Sigma} \widehat{P}_r) + \text{tr}((\widehat{\Sigma} - \Sigma) \widehat{P}_r). \end{aligned}$$

The definition of the eigenvalue problem $\widehat{\Sigma} \widehat{V}_r = \widehat{V}_r \widehat{\Lambda}_r$ gives $\text{tr}(\widehat{\Sigma} \widehat{P}_r) = \text{tr}(\widehat{\Sigma} \widehat{V}_r \widehat{V}_r^\top) = \text{tr}(\widehat{\Lambda}_r)$. Together with $\text{tr}(\Sigma) = \sum_{i=1}^d \lambda_i(\Sigma)$, we have

$$\text{tr}(\widehat{P}_\perp \Sigma \widehat{P}_\perp) = \sum_{i=d_r+1}^d \lambda_i(\Sigma) + \text{tr}(\Lambda_r - \widehat{\Lambda}_r) + \text{tr}((\widehat{\Sigma} - \Sigma) \widehat{P}_r). \quad (26)$$

The term $\text{tr}(\Lambda_r - \widehat{\Lambda}_r)$ satisfies

$$\text{tr}(\Lambda_r - \widehat{\Lambda}_r) \leq \sum_{i=1}^{d_r} |\lambda_i(\Sigma) - \lambda_i(\widehat{\Sigma})| \leq \sqrt{d_r} \left(\sum_{i=1}^{d_r} (\lambda_i(\Sigma) - \lambda_i(\widehat{\Sigma}))^2 \right)^{1/2}.$$

Since Σ and $\widehat{\Sigma}$ are both symmetric, applying Theorem 6.11 of [37], we have

$$\sum_{i=1}^{d_r} (\lambda_i(\Sigma) - \lambda_i(\widehat{\Sigma}))^2 \leq \sum_{i=1}^d (\lambda_i(\Sigma) - \lambda_i(\widehat{\Sigma}))^2 \leq \sum_{i=1}^d \lambda_i(\Sigma - \widehat{\Sigma})^2 = \|\Sigma - \widehat{\Sigma}\|_F^2,$$

which leads to

$$\text{tr}(\Lambda_r - \widehat{\Lambda}_r) \leq \sqrt{d_r} \|\Sigma - \widehat{\Sigma}\|_F. \quad (27)$$

Since for any matrix $A \in \mathbb{R}^{d_r \times d_r}$, it satisfies $\text{tr}(A) \leq \sqrt{d_r} \sqrt{\sum_{i=1}^{d_r} A_{ii}^2} \leq \sqrt{d_r} \|A\|_F$, the term $\text{tr}(\widehat{P}_r (\widehat{\Sigma} - \Sigma))$ satisfies

$$\text{tr}(\widehat{P}_r (\widehat{\Sigma} - \Sigma)) = \text{tr}(\widehat{V}_r^\top (\widehat{\Sigma} - \Sigma) \widehat{V}_r) \leq \sqrt{d_r} \|\widehat{V}_r^\top (\widehat{\Sigma} - \Sigma) \widehat{V}_r\|_F \leq \sqrt{d_r} \|\widehat{\Sigma} - \Sigma\|_F, \quad (28)$$

where the last inequality follows from the property

$$\|AB\|_F^2 = \text{tr}(ABB^\top A^\top) = \text{tr}(BB^\top A^\top A) \leq \|BB^\top\| \text{tr}(A^\top A) = \|B\|^2 \|A\|_F^2.$$

Substituting (27) and (28) into (26), the result of claim 1) follows.

Proof of claim 2). The approximation residual can be expressed as

$$\begin{aligned} \text{tr}(\widehat{P}_\perp \Sigma \widehat{P}_\perp) &= \text{tr}(\widehat{P}_\perp \widehat{\Sigma} \widehat{P}_\perp) + \text{tr}(\widehat{P}_\perp (\Sigma - \widehat{\Sigma}) \widehat{P}_\perp) \\ &= \sum_{i=d_r+1}^d \lambda_i(\widehat{\Sigma}) + \text{tr}(\widehat{P}_\perp (\Sigma - \widehat{\Sigma})) + \text{tr}(\widehat{P}_r (\Sigma - \widehat{\Sigma})) - \text{tr}(\widehat{P}_r (\Sigma - \widehat{\Sigma})) \\ &= \sum_{i=d_r+1}^d \lambda_i(\widehat{\Sigma}) + \text{tr}(\Sigma - \widehat{\Sigma}) + \text{tr}(\widehat{P}_r (\widehat{\Sigma} - \Sigma)). \end{aligned}$$

Applying (28), then the result of claim 2) follows. \square

D.2. Proof of Proposition 4.5

For any i, j -th component of $V(H_0, \nu)$, we have

$$\text{var}_{X \sim \nu} \left[\partial_i \log f(X) \partial_j \log f(X) \frac{\mu(X)}{\nu(X)} \right] \leq \mathbb{E}_{X \sim \nu} \left[\left(\partial_i \log f(X) \partial_j \log f(X) \frac{\mu(X)}{\nu(X)} \right)^2 \right].$$

This way, summing over all indices, we have

$$V(H_0, \nu) \leq \mathbb{E}_{X \sim \nu} \left[\sum_{i,j=1}^d \left(\partial_i \log f(X) \partial_j \log f(X) \frac{\mu(X)}{\nu(X)} \right)^2 \right] = \mathbb{E}_{X \sim \nu} \left[\|\nabla \log f(X)\|^4 \left(\frac{\mu(X)}{\nu(X)} \right)^2 \right].$$

The bound on $V(H_1, \nu)$ can be shown similarly by replacing μ with π . \square

Appendix E: Proofs in Section 5.1

E.1. Proof of Proposition 5.1

We denote the composite transition density of lines 3–5 of Algorithm 1 by $Q(x, x')$. We first verify the detailed balance condition $\pi(x)Q(x, x') = \pi(x')Q(x', x)$. Note that for $x_r \neq x'_r, x_\perp \neq x'_\perp$, the overall transition density is

$$Q(x, x') = p(x_r, x'_r) \beta(x_r, x'_r) \mu(x'_\perp | x'_r) \alpha(x, x').$$

Note that by the formulation of β , the following detailed balance condition holds

$$p(x_r, x'_r) \bar{\varphi}_s(x_r) \beta(x_r, x'_r) = p(x'_r, x_r) \bar{\varphi}_s(x'_r) \beta(x'_r, x_r). \quad (29)$$

These lead to

$$\begin{aligned}
\pi(x)Q(x, x') &= \pi(x)p(x_r, x'_r)\beta(x_r, x'_r)\mu(x'_\perp|x'_r)\alpha(x, x') \\
&= \pi(x)\frac{\bar{\varphi}_s(x'_r)}{\bar{\varphi}_s(x_r)}p(x'_r, x_r)\beta(x'_r, x_r)\mu(x'_\perp|x'_r)\alpha(x, x') \quad (\text{by (29)}) \\
&= p(x'_r, x_r)\beta(x'_r, x_r)\pi(x')\frac{\pi(x)}{\pi(x')}\frac{\bar{\varphi}_s(x'_r)}{\bar{\varphi}_s(x_r)}\mu(x'_\perp|x'_r)\left(1 \wedge \frac{f(x')\bar{\varphi}_s(x_r)\bar{\mu}(x'_r)}{f(x)\bar{\varphi}_s(x'_r)\bar{\mu}(x_r)}\right) \\
&= p(x'_r, x_r)\beta(x'_r, x_r)\pi(x')\frac{f(x)\mu(x)}{f(x')\mu(x')}\frac{\bar{\varphi}_s(x'_r)\mu(x')}{\bar{\varphi}_s(x_r)\bar{\mu}(x'_r)}\left(1 \wedge \frac{f(x')\bar{\varphi}_s(x_r)\bar{\mu}(x'_r)}{f(x)\bar{\varphi}_s(x'_r)\bar{\mu}(x_r)}\right) \\
&= p(x'_r, x_r)\beta(x'_r, x_r)\mu(x_\perp|x_r)\pi(x')\frac{f(x)\bar{\mu}(x_r)\bar{\varphi}_s(x'_r)}{f(x')\bar{\varphi}_s(x_r)\bar{\mu}(x'_r)}\left(1 \wedge \frac{f(x')\bar{\varphi}_s(x_r)\bar{\mu}(x'_r)}{f(x)\bar{\varphi}_s(x'_r)\bar{\mu}(x_r)}\right) \\
&= p(x'_r, x_r)\beta(x'_r, x_r)\mu(x_\perp|x_r)\pi(x')\left(1 \wedge \frac{f(x)\bar{\varphi}_s(x'_r)\bar{\mu}(x_r)}{f(x')\bar{\varphi}_s(x_r)\bar{\mu}(x'_r)}\right) \\
&= p(x'_r, x_r)\beta(x'_r, x_r)\mu(x_\perp|x_r)\pi(x')\alpha(x', x) = \pi(x')Q(x', x).
\end{aligned}$$

For the case $x_r = x'_r, x_\perp \neq x'_\perp$, the overall transition density is

$$Q(x, x') = \delta_{x_r=x'_r}\beta_c(x_r)\mu(x'_\perp|x_r)\alpha(x, x'), \quad \beta_c(x_r) = 1 - \int p(x_r, y_r)\beta(x_r, y_r)dy_r.$$

Therefore, as $x_r = x'_r$, we have

$$\begin{aligned}
\pi(x)Q(x, x') &= \pi(x)\delta_{x_r=x'_r}\beta_c(x_r)\mu(x'_\perp|x_r)\alpha(x, x') \\
&= \delta_{x_r=x'_r}\beta_c(x_r)\frac{\bar{\varphi}_s(x'_r)\bar{\pi}(x_r)}{\bar{\varphi}_s(x_r)\bar{\pi}(x'_r)}\frac{\pi(x)}{\pi(x')}\pi(x')\mu(x'_\perp|x_r)\alpha(x, x') \\
&= \delta_{x_r=x'_r}\beta_c(x_r)\frac{\bar{\varphi}_s(x'_r)\bar{\pi}(x_r)}{\bar{\varphi}_s(x_r)\bar{\pi}(x'_r)}\frac{f(x)\mu(x_\perp|x_r)}{f(x')\mu(x'_\perp|x'_r)}\pi(x')\mu(x'_\perp|x_r)\alpha(x, x') \\
&= \pi(x')\delta_{x_r=x'_r}\beta_c(x_r)\mu(x_\perp|x_r)\alpha(x', x) = \pi(x')Q(x', x).
\end{aligned}$$

Note that if the proposal is rejected for the x_\perp part, then the x_r is also rejected. So the case that $x_r \neq x'_r, x_\perp = x'_\perp$ can be ignored. Finally, the detailed balance condition is trivial if $x = x'$. In conclusion, the detailed balance condition holds, so π is the invariant density of Algorithm 1.

Next, we investigate the acceptance rate of the complement transition. If we denote the MCMC transition probability for the x_r part as

$$P(x_r, x'_r) = p(x_r, x'_r)\beta(x_r, x'_r) + \beta_c(x_r)\delta_{x_r=x'_r}.$$

Note that the acceptance probability can also be written as

$$1 \wedge \frac{f(x')}{f(x)}\frac{\bar{\varphi}_s(x_r)\bar{\mu}(x'_r)}{\bar{\varphi}_s(x'_r)\bar{\mu}(x_r)} = 1 \wedge \frac{f(x')\mu(x')}{f(x)\mu(x)}\frac{\bar{\varphi}_s(x_r)\mu(x_r|x_\perp)}{\bar{\varphi}_s(x'_r)\mu(x'_r|x'_\perp)} = 1 \wedge \frac{\pi(x')\varphi_s(x)}{\pi(x)\varphi_s(x')}.$$

Then, the acceptance rate is given by

$$\mathbb{E}[\alpha(X, X')] = \int \int \pi(x)P(x_r, x'_r)\mu(x'_\perp|x'_r)\left(1 \wedge \frac{\pi(x')\varphi_s(x)}{\pi(x)\varphi_s(x')}\right) dx dx'$$

$$= \int \int P(x_r, x'_r) \mu(x'_\perp | x'_r) \varphi_s(x) \left[\frac{\pi(x)}{\varphi_s(x)} \wedge \frac{\pi(x')}{\varphi_s(x')} \right] dx dx'$$

Therefore if we denote the likelihood ratio $b(x) = \frac{\pi(x)}{\varphi_s(x)}$, then the average rejection probability is

$$1 - \mathbb{E} [\alpha(X, X')] = \int \int P(x_r, x'_r) \varphi_s(x) \mu(x'_\perp | x'_r) [(1 - b(x')) \vee (1 - b(x))] dx dx'.$$

To continue, we note that for any $b \geq 0$, $1 - b \leq 2 - 2\sqrt{b} \leq |2 - 2\sqrt{b}|$, therefore

$$(1 - b(x)) \vee (1 - b(x')) \leq |2 - 2\sqrt{b(x)}| \vee |2 - 2\sqrt{b(x')}| \leq |2 - 2\sqrt{b(x)}| + |2 - 2\sqrt{b'(x)}|.$$

As a consequence,

$$\begin{aligned} 1 - \mathbb{E} [\alpha(X, X')] &\leq \int \int P(x_r, x'_r) \varphi_s(x) \mu(x'_\perp | x'_r) |2 - 2\sqrt{b(x)}| dx dx' \\ &\quad + \int \int P(x_r, x'_r) \varphi_s(x) \mu(x'_\perp | x'_r) |2 - 2\sqrt{b(x')}| dx dx' \\ &= 2 \int \int P(x_r, x'_r) \varphi_s(x) \mu(x'_\perp | x'_r) |2 - 2\sqrt{b(x)}| dx dx' = 4 \int \varphi_s(x) |1 - \sqrt{b(x)}| dx. \end{aligned}$$

Above, the first identity is obtained by observing that $P(x_r, x'_r) \varphi_s(x) \mu(x'_\perp | x'_r) = P(x'_r, x_r) \varphi_s(x') \mu(x_\perp | x_r)$. The second identity is obtained by observing that

$$\int \int P(x_r, x'_r) \mu(x'_\perp | x'_r) dx'_r dx'_\perp = \int P(x_r, x'_r) \left(\int \mu(x'_\perp | x'_r) dx'_\perp \right) dx'_r = \int P(x_r, x'_r) dx'_r = 1.$$

Then by the Cauchy–Schwarz inequality,

$$\int \varphi_s(x) |1 - \sqrt{b(x)}| dx \leq \sqrt{\int \varphi_s(x) (1 - \sqrt{b(x)})^2 dx} \sqrt{\int \varphi_s(x) dx} \leq \sqrt{2} D_H(\pi, \varphi_s).$$

In summary, we have $\mathbb{E} [\alpha(X, X')] \geq 1 - 4\sqrt{2} D_H(\pi, \varphi_s)$. \square

E.2. Proof of Proposition 5.2

Recall that

$$\pi_k(x) = \frac{1}{Z_k} f(x)^{\beta_k} \mu(x), \quad \pi_{k+1}(x) = \frac{1}{Z_{k+1}} f(x)^{\beta_{k+1}} \mu(x),$$

and

$$V_{k+1}(H_1, \pi_k) = \sum_{i,j=1}^d \text{var}_{X \sim \pi_k} \left[\partial_i \log f(X) \partial_j \log f(X) \frac{\pi_{k+1}(X)}{\pi_k(X)} \right].$$

For all x such that $\pi_k(x) > 0$, we have

$$\frac{\pi_{k+1}(x)}{\pi_k(x)} = \frac{Z_k}{Z_{k+1}} f(x)^{(\beta_{k+1} - \beta_k)} = \frac{Z_k}{Z_{k+1}} f(x)^\delta,$$

where $\delta = \beta_{k+1} - \beta_k$. Thus, the variance $V_{k+1}(H_1, \pi_k)$ satisfies

$$\begin{aligned} V_{k+1}(H_1, \pi_k) &= \sum_{i,j=1}^d \text{var}_{X \sim \pi_k} \left[[H^{(k,k+1)}(X)]_{ij} \right] \\ &\leq \sum_{i,j=1}^d \mathbb{E}_{X \sim \pi_k} \left[[H^{(k,k+1)}(X)]_{ij}^2 \right] \\ &= \mathbb{E}_{X \sim \pi_k} \left[\|H^{(k,k+1)}(X)\|_F^2 \right]. \end{aligned} \quad (30)$$

Since the square of the i, j -th component of $H^{(k,k+1)}(x)$ is given by

$$[H^{(k,k+1)}(x)]_{i,j}^2 = \left(\frac{Z_k}{Z_{k+1}} \partial_i \log f(x) \partial_j \log f(x) f(x)^\delta \right)^2,$$

the variance upper bound in (30) can also be expressed as

$$\begin{aligned} \mathbb{E}_{X \sim \pi_k} \left[\|H^{(k,k+1)}(X)\|_F^2 \right] &= \frac{Z_k^2}{Z_{k+1}^2} \sum_{i,j=1}^d \mathbb{E}_{X \sim \pi_k} \left[(\partial_i \log f(X))^2 (\partial_j \log f(X))^2 f(X)^{2\delta} \right] \\ &= \frac{Z_k^2}{Z_{k+1}^2} \int \|\nabla \log f(x)\|^4 f(x)^{2\delta} \pi_k(x) dx \\ &= \frac{Z_k}{Z_{k+1}^2} \int \|\nabla \log f(x)\|^4 f(x)^{2\delta} f(x)^{\beta_k} \mu(x) dx \\ &= \frac{Z_k}{Z_{k+1}^2} \int \|\nabla \log f(x)\|^4 f(x)^{\beta_{k+1} + \delta} \mu(x) dx. \\ &= \frac{Z_k}{Z_{k+1}^2} \int \|\nabla \log f(x)\|^4 f(x)^\delta \pi_{k+1}(x) dx. \end{aligned}$$

Thus, the variance upper bound is finite if $\|\nabla \log f(x)\|^4 f(x)^{\beta_{k+1} + \delta}$ is integrable under μ . \square

Appendix F: Proofs in Section 6

F.1. Proof of Proposition 6.1

For the linear inverse problem, the likelihood function and its log gradient are given by

$$f(x) = \exp\left(-\frac{1}{2}\|Ax - y\|^2\right), \quad \nabla \log f(x) = A^\top(Ax - y).$$

The posterior distribution of X is given by

$$\pi(x) \sim \mathcal{N}((C_A + I)^{-1}u, (C_A + I)^{-1}), \quad C_A = A^\top A, \quad u = A^\top y.$$

Proof of claim 1). The H_0 matrix is given by

$$H_0 = \mathbb{E}_\mu \left[\nabla \log f(X) \nabla \log f(X)^\top \right] = A^\top (AA^\top + yy^\top) A = C_A^2 + U,$$

where $U = A^\top yy^\top A$ is a rank 1 matrix. Apply Lemma A.3 with $H_0 = C_A^2 + U$, we have

$$\lambda_{k+1}(H_0) \leq \lambda_k(C_A^2).$$

Proof of claim 2). The H_1 matrix is given by

$$H_1 = \mathbb{E}_\pi \left[\nabla \log f(X) \nabla \log f(X)^\top \right] = \mathbb{E}_\pi \left[A^\top (AX - y)(AX - y)^\top A \right].$$

For a given y and $X \sim \pi$, the vector $A^\top (AX - y)$ follows a Gaussian distribution with the mean

$$A^\top \left(A(C_A + I)^{-1}u - y \right) = C_A(C_A + I)^{-1}u - A^\top y = C_A(C_A + I)^{-1}u - u = -(C_A + I)^{-1}u$$

and the covariance $C_A(C_A + I)^{-1}C_A$. This way, we have

$$H_1 = C_A(C_A + I)^{-1}C_A + (C_A + I)^{-1}U(C_A + I)^{-1},$$

where $(C_A + I)^{-1}U(C_A + I)^{-1}$ is a rank-1 matrix. Thus, by Lemma A.3, we have

$$\lambda_{k+1}(H_1) \leq \lambda_k(C_A(C_A + I)^{-1}C_A).$$

Finally note that eigenvectors of $C_A(I + C_A)^{-1}C_A$ are identical with the eigenvectors of C_A , with

$$v_k^\top C_A(I + C_A)^{-1}C_A v_k = \frac{\lambda_k(C_A)^2}{1 + \lambda_k(C_A)},$$

and we have our claim.

Proof of claim 3). Note that for a fixed y , the normalizing constant Z is the integral

$$Z = \int (2\pi)^{-d/2} \exp \left(-\frac{1}{2} \|Ax - y\|^2 - \frac{1}{2} \|x\|^2 \right) dx,$$

which is equivalent to

$$(2\pi)^{-d_y/2} Z = \int (2\pi)^{-d/2-d_y/2} \exp \left(-\frac{1}{2} \|Ax - y\|^2 - \frac{1}{2} \|x\|^2 \right) dx,$$

where the integrand of the right hand side is the joint probability density of x and y . In other words, if we view $(2\pi)^{-d_y/2} Z$ as a function of y , then the right-hand side of the equation above is the marginal probability density of y . Since the marginal of a Gaussian distribution is still Gaussian, it is easy to see that y follows the Gaussian distribution $\mathcal{N}(0, I + AA^\top)$. Thus, we have

$$Z = \det(I + AA^\top)^{-1/2} \exp \left(-\frac{1}{2} y^\top (I + AA^\top)^{-1} y \right).$$

Since $\det(I + AA^\top) = \det(I + A^\top A) = \det(I + C_A)$, we have

$$\frac{1}{\sqrt{\det(I + C_A)}} \geq Z \geq \frac{1}{\sqrt{\det(I + C_A)}} \exp \left(-\frac{1}{2} \|y\|^2 \right).$$

Then, the result follows.

Proof of claim 4). We have

$$\begin{aligned}\|f\|_{2,\mu}^2 &= (2\pi)^{-d/2} \int \exp\left(-\|Ax - y\|^2 - \frac{1}{2}\|x\|^2\right) dx \\ &= (2\pi)^{d_y/2} \left[(2\pi)^{-d/2-d_y/2} \int \exp\left(-\frac{1}{2}\|\tilde{A}x - \tilde{y}\|^2 - \frac{1}{2}\|x\|^2\right) dx \right]\end{aligned}$$

with $\tilde{A} = \sqrt{2}A$ and $\tilde{y} = \sqrt{2}y$. Note that the term inside the square brackets is the normalizing constant of the posterior defined by the prior $\mathcal{N}(0, I_d)$, the parameter-to-observable map \tilde{A} , and the data \tilde{y} . This way, applying a similar identity to that in claim 3), we have

$$\begin{aligned}\|f\|_{2,\mu}^2 &= \det(I + \tilde{A}\tilde{A}^\top)^{-1/2} \exp\left(-\frac{1}{2}\tilde{y}^\top(I + \tilde{A}\tilde{A}^\top)^{-1}\tilde{y}\right) \\ &= \frac{1}{\sqrt{\det(I + 2C_A)}} \exp\left(-y^\top(I + 2AA^\top)^{-1}y\right).\end{aligned}$$

This leads to

$$\frac{\|f\|_{2,\mu}}{Z} = \frac{\det(I + C_A)^{1/2}}{\det(I + 2C_A)^{1/4}} \exp\left(\frac{1}{2}y^\top(I + AA^\top)^{-1}y - \frac{1}{2}y^\top(I + 2AA^\top)^{-1}y\right). \quad (31)$$

Suppose the eigenvalue decomposition of AA^\top is given by $AA^\top = U\Lambda U^\top$, then

$$\begin{aligned}(I + AA^\top)^{-1} - (I + 2AA^\top)^{-1} &= U(I + \Lambda)^{-1}U^\top - U(I + 2\Lambda)^{-1}U^\top \\ &= U\Lambda(I + \Lambda)^{-1}(I + 2\Lambda)^{-1}U^\top.\end{aligned}$$

Therefore if AA^\top has an eigenvector u_i so that $AA^\top u_i = \lambda_i u_i$, then it is also an eigenvector of $(I + AA^\top)^{-1} - (I + 2AA^\top)^{-1}$:

$$((I + AA^\top)^{-1} - (I + 2AA^\top)^{-1})u_i = \frac{\lambda_i}{(1 + \lambda_i)(1 + 2\lambda_i)}u_i.$$

Since $\frac{\lambda_i}{(1 + \lambda_i)(1 + 2\lambda_i)} = \frac{1}{2\lambda_i + 1/\lambda_i + 3} \leq \frac{\sqrt{2}-1}{2(\sqrt{2}+1)}$, we obtain the upper bound following (31)

$$\begin{aligned}\frac{\|f\|_{2,\mu}}{Z} &\leq \left(\prod_{k=1}^d \frac{1 + 2\lambda_k(C_A) + \lambda_k(C_A)^2}{1 + 2\lambda_k(C_A)}\right)^{1/4} \exp\left(\frac{\sqrt{2}-1}{2(\sqrt{2}+1)}\|y\|^2\right) \\ &\leq \prod_{k=1}^d \left(1 + \lambda_k(C_A)^2\right)^{1/4} \exp\left(\frac{\sqrt{2}-1}{2(\sqrt{2}+1)}\|y\|^2\right) \\ &= \det(I + C_A^2)^{1/4} \exp\left(\frac{\sqrt{2}-1}{2(\sqrt{2}+1)}\|y\|^2\right) \\ &= \det(I + C_A^2)^{1/4} \exp\left(\frac{1}{2}(\sqrt{2}-1)^2\|y\|^2\right).\end{aligned}$$

Proof of claim 5). Recall that $\nabla \log f(x) = A^\top (Ax - y)$. We introduce the random variable $\zeta = A^\top AX - A^\top y$ that follows the Gaussian distribution $p(\zeta) = \mathcal{N}(-A^\top y, C_A^2)$. Employing the upper bound established in Proposition 4.5, we have

$$V(H_0, \mu) \leq \mathbb{E}_\mu \left[\|\nabla \log f(X)\|^4 \right] = \mathbb{E}_{\zeta \sim p} \left[\left(\sum_{i=1}^d \zeta_i^2 \right)^2 \right] = \mathbb{E}_{\zeta \sim p} \left[\sum_{i,j} \zeta_i^2 \zeta_j^2 \right].$$

Note that if $X \sim \mathcal{N}(m, \sigma^2)$, we can write it as $X = m + \sigma Z$ where $Z \sim \mathcal{N}(0, 1)$. With this we find that

$$\mathbb{E}X^4 = m^4 + 2\sigma^2 m^2 + 3\sigma^4 \leq 3(m^2 + \sigma^2)^2 = 3(\mathbb{E}X^2)^2.$$

For $i = j$, we have $\mathbb{E}[\zeta_i^4] = 3(\mathbb{E}[\zeta_i^2])^2$ because ζ_i is Gaussian distributed and all real-valued Gaussian random variables have zero excess kurtosis, and for $i \neq j$, we have $\mathbb{E}[\zeta_i^2 \zeta_j^2] \leq \sqrt{\mathbb{E}[\zeta_i^4] \mathbb{E}[\zeta_j^4]} = 3\mathbb{E}[\zeta_i^2] \mathbb{E}[\zeta_j^2]$. This leads to

$$\mathbb{E}_{\zeta \sim p} [\|\zeta\|^4] = \mathbb{E}_{\zeta \sim p} \left[\sum_{i,j} \zeta_i^2 \zeta_j^2 \right] \leq 3 \sum_{i,j} \mathbb{E}[\zeta_i^2] \mathbb{E}[\zeta_j^2] = 3 \left(\sum_i \mathbb{E}[\zeta_i^2] \right)^2. \quad (32)$$

Since $\zeta \sim \mathcal{N}(-A^\top y, C_A^2)$, we have

$$\sum_i \mathbb{E}[\zeta_i^2] = \text{tr}(C_A^2) + \text{tr}(A^\top y y^\top A) = \sum_{i=1}^d \lambda_i(C_A)^2 + \|A^\top y\|^2.$$

Thus, we have

$$V(H_0, \mu) \leq 3 \left(\sum_{i=1}^d \lambda_i(C_A)^2 + \|A^\top y\|^2 \right)^2 \leq 6 \left(\sum_{i=1}^d \lambda_i(C_A)^2 \right)^2 + 6 \|A^\top y\|^4.$$

For the case $k = 1$, employing the upper bound established in Proposition 4.5, we have

$$V(H_1, \mu) \leq \mathbb{E}_\mu \left[\|\nabla \log f(X)\|^4 \frac{\pi(X)^2}{\mu(X)^2} \right] = \frac{1}{Z_2} \int \|\nabla \log f(x)\|^4 f(x)^2 \mu(x) dx.$$

Define a new distribution with the density

$$\begin{aligned} \pi_2(x) &= \frac{1}{Z_2} f(x)^2 \mu(x) \propto \exp \left(-\|Ax - y\| - \frac{1}{2} \|x\|^2 \right) \\ &\propto \exp \left(-\frac{1}{2} x^\top (I + 2A^\top A) x - y^\top Ax \right). \end{aligned} \quad (33)$$

Clearly π_2 is a Gaussian distribution, its mean is $2(I + 2C_A)^{-1} A^\top y$, its covariance is $(I + 2C_A)^{-1}$, and the normalizing constant $Z_2 = \|f\|_{2,\mu}^2$ satisfies

$$\frac{Z_2}{Z^2} \leq \prod_{k=1}^d \left(1 + \lambda_k(C_A)^2 \right)^{1/2} \exp \left(\frac{\sqrt{2}-1}{\sqrt{2}+1} \|y\|^2 \right) = \sqrt{\det(I + C_A^2)} \exp \left((\sqrt{2}-1)^2 \|y\|^2 \right),$$

as the result of claim 4). We express the upper bound on the variance as

$$V(H_1, \mu) \leq \mathbb{E}_\mu \left[\|\nabla \log f(X)\|^4 \frac{\pi(X)^2}{\mu(X)^2} \right] = \frac{Z_2}{Z^2} \mathbb{E}_{\pi_2} \left[\|\nabla \log f(X)\|^4 \right] = \frac{Z_2}{Z^2} \mathbb{E}_{\pi_2} \left[\|C_A X - A^\top y\|^4 \right].$$

Similar to the proof of the first part, we can introduce $\zeta = C_A X - A^\top y$, for $X \sim \pi_2$. Then ζ follows the Gaussian distribution with the mean

$$2C_A(I + 2C_A)^{-1}A^\top y - A^\top y = -(I + 2C_A)^{-1}A^\top y,$$

and the covariance $C_A(I + 2C_A)^{-1}C_A$. This leads to

$$\begin{aligned} \sum_i^d \mathbb{E}[\zeta_i^2] &= \text{tr}(C_A(I + 2C_A)^{-1}C_A) + \|(I + 2C_A)^{-1}A^\top y\|^2 \\ &= \sum_{i=1}^d \frac{\lambda_i(C_A)^2}{1 + 2\lambda_i(C_A)} + \|(I + 2C_A)^{-1}A^\top y\|^2 \\ &\leq \sum_{i=1}^d \frac{\lambda_i(C_A)^2}{1 + 2\lambda_i(C_A)} + \|A^\top y\|^2. \end{aligned} \quad (34)$$

Thus, following a similar derivation to the case $k = 0$, we have

$$V(H_1, \mu) \leq 6\sqrt{\det(I + C_A^2)} \exp\left((\sqrt{2} - 1)^2 \|y\|^2\right) \left(\left(\sum_{i=1}^d \frac{\lambda_i(C_A)^2}{1 + 2\lambda_i(C_A)} \right)^2 + \|A^\top y\|^4 \right).$$

Proof of claim 6). Consider the tempered target density

$$\pi_\beta(x) = \frac{1}{Z_\beta} f(x)^\beta \mu(x) = \frac{1}{(2\pi)^{d/2} Z_\beta} \exp\left(-\frac{1}{2} \|\sqrt{\beta}Ax - \sqrt{\beta}y\|^2 - \frac{1}{2} \|x\|^2\right),$$

where the normalizing constant takes the form

$$Z_\beta = \det(I + \beta AA^\top)^{-1/2} \exp\left(-\frac{\beta}{2} y^\top (I + \beta AA^\top)^{-1} y\right). \quad (35)$$

We use the shorthand notations π_k and Z_k to denote π_{β_k} and Z_{β_k} , respectively. Let $\delta = \beta_{k+1} - \beta_k$, we have

$$\begin{aligned} V_{k+1}(H_1, \pi_k) &\leq \frac{Z_k^2}{Z_{k+1}^2} \mathbb{E}_{\pi_k} \left[\|\nabla \log f(X)\|^4 f(X)^{2\delta} \right] \\ &= \frac{Z_k}{Z_{k+1}^2} \mathbb{E}_\mu \left[\|\nabla \log f(X)\|^4 f(X)^{2\delta + \beta_k} \right]. \end{aligned}$$

Following a similar procedure in the proof of claim 5), we define a new distribution with the density

$$\pi_\tau(x) = \frac{1}{Z_\tau} f(x)^\tau \mu(x) dx,$$

where $\tau = 2\delta + \beta_k = 2\beta_{k+1} - \beta_k = \beta_{k+1} + \delta$. The density $\pi_\tau(x)$ has the mean $\tau(I + \tau C_A)^{-1} A^\top y$ and the covariance $(I + \tau C_A)^{-1}$. We express the upper bound on the variance as

$$\begin{aligned} V_{k+1}(H_1, \mu) &\leq \frac{Z_k}{Z_{k+1}^2} \mathbb{E}_\mu \left[\|\nabla \log f(X)\|^4 f(X)^\tau \right] \\ &= \frac{Z_\tau Z_k}{Z_{k+1}^2} \mathbb{E}_{\pi_\tau} \left[\|\nabla \log f(X)\|^4 \right] \\ &= \frac{Z_\tau Z_k}{Z_{k+1}^2} \mathbb{E}_{\pi_\tau} \left[\|C_A X - A^\top y\|^4 \right]. \end{aligned} \quad (36)$$

Then, for $X \sim \pi_\tau$, we introduce $\zeta = C_A X - A^\top y$, which follows the Gaussian distribution with the mean

$$\mathbb{E}[\zeta] = (\tau C_A (I + \tau C_A)^{-1} - I) A^\top y = -(I + \tau C_A)^{-1} A^\top y,$$

and the covariance $C_A (I + \tau C_A)^{-1} C_A$. Similar to the derivation of (34), this leads to

$$\begin{aligned} \sum_{i=1}^d \mathbb{E}[\zeta_i^2] &= \mathbb{E}[\|\zeta\|^2] = \|\mathbb{E}[\zeta]\|^2 + \text{tr}(\text{cov}[\zeta]) \\ &= \text{tr}(C_A (I + \tau C_A)^{-1} C_A) + \|(I + \tau C_A)^{-1} A^\top y\|^2 \\ &\leq \sum_{i=1}^d \frac{\lambda_i(C_A)^2}{1 + \tau \lambda_i(C_A)} + \|A^\top y\|^2, \end{aligned}$$

which yields the following using the same argument used in (32):

$$\mathbb{E}_{\pi_\tau} \left[\|C_A X - A^\top y\|^4 \right] = \mathbb{E}_{\pi_\tau} \left[\|\zeta\|^4 \right] \leq 6 \left(\left(\sum_{i=1}^d \frac{\lambda_i(C_A)^2}{1 + \tau \lambda_i(C_A)} \right)^2 + \|A^\top y\|^4 \right). \quad (37)$$

Recalling (35), the ratio between normalizing constants in (36) can be expressed as

$$\frac{Z_\tau Z_k}{Z_{k+1}^2} = \frac{\det(I + \beta_{k+1} A A^\top)}{\sqrt{\det(I + \beta_k A A^\top) \det(I + \tau A A^\top)}} \exp\left(\frac{1}{2} y^\top T y\right),$$

where

$$T = 2\beta_{k+1}(I + \beta_{k+1} A A^\top)^{-1} - \beta_k(I + \beta_k A A^\top)^{-1} - \tau(I + \tau A A^\top)^{-1}.$$

In the above equation, the ratio between determinants can be expressed as

$$\frac{\det(I + \beta_{k+1} A A^\top)}{\sqrt{\det(I + \beta_k A A^\top) \det(I + \tau A A^\top)}} = \left(\prod_{i=1}^d \frac{1 + 2\beta_{k+1} \lambda_i(C_A) + \beta_{k+1}^2 \lambda_i(C_A)^2}{1 + 2\beta_k \lambda_i(C_A) + \beta_k \tau \lambda_i(C_A)^2} \right)^{1/2}.$$

Since $\beta_{k+1}^2 - (\beta_{k+1} - \beta_k)^2 = \beta_k(2\beta_{k+1} - \beta_k)$, which gives $\beta_{k+1}^2 = \delta^2 + \beta_k \tau$, and thus

$$\frac{\det(I + \beta_{k+1} A A^\top)}{\sqrt{\det(I + \beta_k A A^\top) \det(I + \tau A A^\top)}} = \prod_{i=1}^d \left(1 + \frac{\delta^2 \lambda_i(C_A)^2}{1 + 2\beta_{k+1} \lambda_i(C_A) + \beta_k \tau \lambda_i(C_A)^2} \right)^{1/2}$$

$$\leq \prod_{i=1}^d \left(1 + \delta^2 \lambda_i(C_A)^2\right)^{1/2}. \quad (38)$$

Since the matrix T and the matrix AA^\top share the same eigenvectors, the eigenvalues of T can be expressed as

$$\begin{aligned} \lambda_i(T) &= \frac{\beta_k}{1 + \beta_{k+1} \lambda_i(AA^\top)} - \frac{\beta_k}{1 + \beta_k \lambda_i(AA^\top)} + \frac{\tau}{1 + \beta_{k+1} \lambda_i(AA^\top)} - \frac{\tau}{1 + \tau \lambda_i(AA^\top)} \\ &= \frac{-\beta_k \delta \lambda_i(AA^\top)}{(1 + \beta_{k+1} \lambda_i(AA^\top))(1 + \beta_k \lambda_i(AA^\top))} + \frac{\tau \delta \lambda_i(AA^\top)}{(1 + \beta_{k+1} \lambda_i(AA^\top))(1 + \tau \lambda_i(AA^\top))} \\ &= \frac{\delta \lambda_i(AA^\top)}{1 + \beta_{k+1} \lambda_i(AA^\top)} \left(\frac{\tau}{1 + \tau \lambda_i(AA^\top)} - \frac{\beta_k}{1 + \beta_k \lambda_i(AA^\top)} \right) \\ &= \frac{2\delta^2 \lambda_i(AA^\top)}{(1 + \beta_{k+1} \lambda_i(AA^\top))(1 + \tau \lambda_i(AA^\top))(1 + \beta_k \lambda_i(AA^\top))}. \end{aligned}$$

This way, we have $\lambda_i(T) \leq 2\delta^2 \lambda_i(AA^\top)$, and thus $T \preceq 2\delta^2 AA^\top$. This leads to

$$\exp\left(\frac{1}{2} y^\top T y\right) \leq \exp\left(\delta^2 \|A^\top y\|^2\right).$$

Substituting the above inequality, (37), and (38) into (36), we have

$$V_{k+1}(H_1, \mu) \leq 6 \sqrt{\det(I + \delta^2 C_A^2)} \exp\left(\delta^2 \|A^\top y\|^2\right) \left(\left(\sum_{i=1}^d \frac{\lambda_i(C_A)^2}{1 + \tau \lambda_i(C_A)} \right)^2 + \|A^\top y\|^4 \right).$$

□

F.2. Proof of Corollary 6.2

We will first show that the eigenvalues of C_A are bounded by those of Γ . By the Courant–Fischer–Weyl min-max principle, we note that for any symmetric matrix C

$$\lambda_r(C) = \min_V \left\{ \max_{x \in V} \{x^\top C x, \|x\| = 1\}, \dim(V) = d - r + 1 \right\}.$$

Let the eigenvectors of Γ be v_1, \dots, v_d . Now we pick $V = \text{span}\{v_r, \dots, v_d\}$. Then for any $x \in V$ of unit ℓ^2 norm,

$$x^\top C_A x = x^\top \Gamma^{1/2} G^\top G \Gamma^{1/2} x = \|\Gamma^{1/2} x\|^2 \leq \|G\|^2 \|\Gamma^{1/2} x\|^2 \leq \|G\|^2 \lambda_r(\Gamma).$$

Therefore, $\lambda_r(C_A) \leq \|G\|^2 \lambda_r(\Gamma)$.

The following identities are useful: For $r \geq 2$, we have

$$\sum_{j=r}^d j^{-\alpha} \leq \int_{r-1}^{\infty} x^{-\alpha} dx \leq \frac{(r-1)^{1-\alpha}}{\alpha-1},$$

and for $r = 1$, we have

$$1 + \sum_{j=2}^d j^{-\alpha} \leq \frac{\alpha}{\alpha - 1}.$$

For any $a > 0$, we have

$$\begin{aligned} \prod_{j=r}^d (1 + a\lambda_j(C_A)) &\leq \prod_{j=r}^d (1 + a\|G\|^2 \lambda_j(\Gamma)) \\ &\leq \exp\left(a\|G\|^2 \sum_{j=r}^d \lambda_j(\Gamma)\right) = \exp\left(a\|G\|^2 C_\Gamma \sum_{j=r}^d j^{-\alpha}\right). \end{aligned}$$

Thus, we have

$$\sum_{i=1}^d \lambda_i(C_A)^2 \leq \|G\|^4 C_\Gamma^2 \frac{2\alpha}{2\alpha - 1}, \quad (39)$$

and

$$\det(I + aC_A^2) \leq \exp\left(a\|G\|^4 C_\Gamma^2 \frac{2\alpha}{2\alpha - 1}\right). \quad (40)$$

Then, replacing the estimates in Proposition 6.1 with these upper bounds, the results follow. \square

Acknowledgments

X. Tong's research is supported by MOE Academic Research Funds R-146-000-292-114. T. Cui acknowledges support from the Australian Research Council.

References

- [1] AGAPIOU, S., DASHTI, M. and HELIN, T. (2018). Rates of contraction of posterior distributions based on p -exponential priors. *arXiv preprint arXiv:1811.12244*.
- [2] AGAPIOU, S., PAPASPILIOPOULOS, O., SANZ-ALONSO, D., STUART, A. et al. (2017). Importance sampling: Intrinsic dimension and computational cost. *Statistical Science* **32** 405–431.
- [3] AGAPIOU, S., ROBERTS, G. O., VOLLMER, S. J. et al. (2018). Unbiased Monte Carlo: Posterior estimation for intractable/infinite-dimensional models. *Bernoulli* **24** 1726–1786.
- [4] ANDRIEU, C. and ROBERTS, G. O. (2009). The pseudo-marginal approach for efficient Monte Carlo computations. *The Annals of Statistics* **37** 697–725.
- [5] ANDRIEU, C. and VIHOLA, M. (2015). Convergence properties of pseudo-marginal Markov chain Monte Carlo algorithms. *Ann. Appl. Probab.* **25** 1030–1077.
- [6] BESKOS, A., CRISAN, D., JASRA, A. et al. (2014). On the stability of sequential Monte Carlo methods in high dimensions. *The Annals of Applied Probability* **24** 1396–1445.
- [7] BESKOS, A., GIROLAMI, M., LAN, S., FARRELL, P. E. and STUART, A. M. (2017). Geometric MCMC for infinite-dimensional inverse problems. *Journal of Computational Physics* **335** 327–351.

- [8] BESKOS, A., JASRA, A., LAW, K., MARZOUK, Y. and ZHOU, Y. (2018). Multilevel sequential Monte Carlo with dimension-independent likelihood-informed proposals. *SIAM/ASA Journal on Uncertainty Quantification* **6** 762–786.
- [9] BIGONI, D., ZAHM, O., SPANTINI, A. and MARZOUK, Y. (2019). Greedy inference with layers of lazy maps. *arXiv preprint arXiv:1906.00031*.
- [10] BOBKOV, S. G. (1999). Isoperimetric and analytic inequalities for log-concave probability measures. *The Annals of Probability* **27** 1903–1921.
- [11] BOBKOV, S. and LEDOUX, M. (1997). Poincaré’s inequalities and Talagrand’s concentration phenomenon for the exponential distribution. *Probability Theory and Related Fields* **107** 383–400.
- [12] BOBKOV, S. G. and LEDOUX, M. (2000). From Brunn-Minkowski to Brascamp-Lieb and to logarithmic sobolev inequalities. *Geometric & Functional Analysis GFA* **10** 1028–1052.
- [13] BOBKOV, S. G. and LEDOUX, M. (2009). Weighted Poincaré-type inequalities for Cauchy and other convex measures. *The Annals of Probability* **37** 403–427.
- [14] BOLLEY, F. and VILLANI, C. (2005). Weighted Csiszár-Kullback-Pinsker inequalities and applications to transportation inequalities. In *Annales de la Faculté des sciences de Toulouse: Mathématiques* **14** 331–352.
- [15] BRASCAMP, H. J. and LIEB, E. H. (1976). On extensions of the Brunn-Minkowski and Prékopa-Leindler theorems, including inequalities for log concave functions, and with an application to the diffusion equation. *Journal of Functional Analysis* **22** 366–389.
- [16] BUI-THANH, T., BURSTEDDE, C., GHATTAS, O., MARTIN, J., STADLER, G. and WILCOX, L. C. (2012). Extreme-scale UQ for Bayesian inverse problems governed by PDEs. In *SC’12: Proceedings of the International Conference on High Performance Computing, Networking, Storage and Analysis* 1–11. IEEE.
- [17] BUI-THANH, T., GHATTAS, O., MARTIN, J. and STADLER, G. (2013). A computational framework for infinite-dimensional Bayesian inverse problems Part I: The linearized case, with application to global seismic inversion. *SIAM Journal on Scientific Computing* **35** A2494–A2523.
- [18] CAI, T. and HALL, P. (2008). Prediction in function linear regression. *Ann. Statist.* **34** 2159–2179.
- [19] CONSTANTINE, P. G., KENT, C. and BUI-THANH, T. (2016). Accelerating Markov chain Monte Carlo with active subspaces. *SIAM Journal on Scientific Computing* **38** A2779–A2805.
- [20] COTTER, S. L., ROBERTS, G. O., STUART, A. M. and WHITE, D. (2013). MCMC methods for functions: modifying old algorithms to make them faster. *Statistical Science* 424–446.
- [21] CUI, T. and DOLGOV, S. (2020). Deep Composition of Tensor Trains using Squared Inverse Rosenblatt Transports. *arXiv preprint arXiv:2007.06968*.
- [22] CUI, T., FOX, C. and O’SULLIVAN, M. J. (2011). Bayesian calibration of a large-scale geothermal reservoir model by a new adaptive delayed acceptance Metropolis Hastings algorithm. *Water Resources Research* **47**.
- [23] CUI, T., LAW, K. J. H. and MARZOUK, Y. M. (2016). Dimension-independent likelihood-informed MCMC. *J. Comput. Phys.* **304** 109–137.
- [24] CUI, T. and ZAHM, O. (2020). Data-Free Likelihood-Informed Dimension Reduction of Bayesian Inverse Problems. *hal preprint: hal-02938064*.
- [25] CUI, T., MARTIN, J., MARZOUK, Y. M., SOLONEN, A. and SPANTINI, A. (2014). Likelihood-informed dimension reduction for nonlinear inverse problems. *Inverse Problems* **30** 114015.
- [26] DASHTI, M. and STUART, A. M. (2011). Uncertainty quantification and weak approximation of an elliptic inverse problem. *SIAM Journal on Numerical Analysis* **49** 2524–2542.
- [27] DETOMMASO, G., CUI, T., MARZOUK, Y., SPANTINI, A. and SCHEICHL, R. (2018). A Stein variational Newton method. *Advances in Neural Information Processing Systems* **31** 9169–9179.

- [28] DODWELL, T. J., KETELSEN, C., SCHEICHL, R. and TECKENTRUP, A. L. (2019). Multilevel markov chain monte carlo. *Siam Review* **61** 509–545.
- [29] DRINEAS, P. and IPSEN, I. C. (2019). Low-rank matrix approximations do not need a singular value gap. *SIAM Journal on Matrix Analysis and Applications* **40** 299–319.
- [30] FLATH, H. P., WILCOX, L. C., AKÇELIK, V., HILL, J., VAN BLOEMEN WAANDER, B. and GHATTAS, O. (2011). Fast Algorithms for Bayesian Uncertainty Quantification in Large-Scale Linear Inverse Problems Based on Low-Rank Partial Hessian Approximations. *SIAM J. Sci. Comput.* **33** 407–432.
- [31] GROSS, L. (1975). Logarithmic sobolev inequalities. *American Journal of Mathematics* **97** 1061–1083.
- [32] HAARIO, H., LAINE, M., LEHTINEN, M., SAKSMAN, E. and TAMMINEN, J. (2004). Markov chain Monte Carlo methods for high dimensional inversion in remote sensing. *Journal of the Royal Statistical Society: series B (statistical methodology)* **66** 591–607.
- [33] HALL, P. and HOROWITZ, J. L. (2007). Methodology and convergence rates for functional linear regression. *Ann. Statist.* **35** 70–91.
- [34] IGLESIAS, M. A., LIN, K. and STUART, A. M. (2014). Well-posed Bayesian geometric inverse problems arising in subsurface flow. *Inverse Problems* **30** 114001.
- [35] KAIPIO, J. P., KOLEHMAINEN, V., SOMERSALO, E. and VAUHKONEN, M. (2000). Statistical inversion and Monte Carlo sampling methods in electrical impedance tomography. *Inverse problems* **16** 1487.
- [36] KARHUNEN, K. (1947). Über lineare Methoden in der Wahrscheinlichkeitsrechnung. *Ann. Acad. Sci. Fennicae. Ser. A. I. Math.-Phys* **37** 1–79.
- [37] KATO, T. (1982). *A Short Introduction to Perturbation Theory for Linear Operators*. Springer-Verlag.
- [38] LEDOUX, M. (1994). A simple analytic proof of an inequality by P. Buser. *Proceedings of the American mathematical society* **121** 951–959.
- [39] LIE, H. C., SULLIVAN, T. J. and TECKENTRUP, A. (2019). Error bounds for some approximate posterior measures in Bayesian inference. *arXiv preprint arXiv:1911.05669*.
- [40] LIU, Q. and WANG, D. (2016). Stein variational gradient descent: A general purpose bayesian inference algorithm. *Advances in neural information processing systems* **29** 2378–2386.
- [41] LOËVE, M. (1978). *Probability theory, Vol. II*, 4 ed. *Graduate Texts in Mathematics* **46**. Springer-Verlag, Berlin.
- [42] MARTIN, J., WILCOX, L. C., BURSTEDDE, C. and GHATTAS, O. (2012). A stochastic Newton MCMC method for large-scale statistical inverse problems with application to seismic inversion. *SIAM Journal on Scientific Computing* **34** A1460–A1487.
- [43] MARZOUK, Y., MOSELHY, T., PARNO, M. and SPANTINI, A. (2016). Sampling via measure transport: An introduction. *Handbook of uncertainty quantification* 1–41.
- [44] MENZ, G., SCHLICHTING, A. et al. (2014). Poincaré and logarithmic Sobolev inequalities by decomposition of the energy landscape. *Annals of Probability* **42** 1809–1884.
- [45] MORZFELD, M., TONG, X. T. and MARZOUK, Y. M. (2019). Localization for MCMC: sampling high-dimensional posterior distributions with local structure. *Journal of Computational Physics* **380** 1–28.
- [46] MURRAY, I., MACKAY, D. and ADAMS, R. P. (2008). The Gaussian process density sampler. *Advances in Neural Information Processing Systems* **21** 9–16.
- [47] OTTO, F. and VILLANI, C. (2000). Generalization of an inequality by Talagrand and links with the logarithmic Sobolev inequality. *Journal of Functional Analysis* **173** 361–400.
- [48] PARENTE, M. T., WALLIN, J., WOHLMUTH, B. et al. (2020). Generalized bounds for active subspaces. *Electronic Journal of Statistics* **14** 917–943.

- [49] PETRA, N., MARTIN, J., STADLER, G. and GHATTAS, O. (2014). A computational framework for infinite-dimensional Bayesian inverse problems, Part II: Stochastic Newton MCMC with application to ice sheet flow inverse problems. *SIAM Journal on Scientific Computing* **36** A1525–A1555.
- [50] RAMSAY, J. O. and SILVERMAN, B. W. (2005). *Functional data analysis (2nd ed.)*. Springer.
- [51] RUDOLF, D. and SPRUNGK, B. (2018). On a generalization of the preconditioned Crank–Nicolson Metropolis algorithm. *Foundations of Computational Mathematics* **18** 309–343.
- [52] SANZ-ALONSO, D. (2018). Importance sampling and necessary sample size: an information theory approach. *SIAM/ASA Journal on Uncertainty Quantification* **6** 867–879.
- [53] SPANTINI, A., BIGONI, D. and MARZOUK, Y. (2018). Inference via low-dimensional couplings. *The Journal of Machine Learning Research* **19** 2639–2709.
- [54] SPANTINI, A., SOLOMON, A., CUI, T., MARTIN, J., TENORIO, L. and MARZOUK, Y. (2015). Optimal low-rank approximations of Bayesian linear inverse problems. *SIAM Journal on Scientific Computing* **37** A2451–A2487.
- [55] STEERNEMAN, T. (1983). On the total variation and Hellinger distance between signed measures; an application to product measures. *Proceedings of the American Mathematical Society* **88** 684–688.
- [56] STEWART, G. W. (1980). The efficient generation of random orthogonal matrices with an application to condition estimators. *SIAM Journal on Numerical Analysis* **17** 403–409.
- [57] STUART, A. (2010). Inverse problems: a Bayesian perspective. *Acta numerica* **19** 451–559.
- [58] SULLIVAN, T. J. (2015). *Introduction to uncertainty quantification* **63**. Springer.
- [59] TABAK, E. G., TRIGILA, G. and ZHAO, W. (2020). Conditional density estimation and simulation through optimal transport. *Machine Learning* 1–24.
- [60] TABAK, E. G. and TURNER, C. V. (2013). A family of nonparametric density estimation algorithms. *Communications on Pure and Applied Mathematics* **66** 145–164.
- [61] TONG, X. T., MORZFELD, M. and MARZOUK, Y. M. (2020). MALA-within-Gibbs samplers for high-dimensional distributions with sparse conditional structure. *SIAM Journal on Scientific Computing* **42** A1765–A1788.
- [62] TRIGILA, G. and TABAK, E. G. (2016). Data-driven optimal transport. *Communications on Pure and Applied Mathematics* **69** 613–648.
- [63] TSYBAKOV, A. B. (2008). *Introduction to nonparametric estimation*. Springer Science & Business Media.
- [64] YU, Y., WANG, T. and SAMWORTH, R. J. (2015). A useful variant of the Davis–Kahan theorem for statisticians. *Biometrika* **102** 315–323.
- [65] ZAHM, O., CUI, T., LAW, K., SPANTINI, A. and MARZOUK, Y. (2018). Certified dimension reduction in nonlinear Bayesian inverse problems. *arXiv preprint arXiv:1807.03712*.